NAVY DEPARTMENT

THE DAVID W. TAYLOR MODEL BASIN

WASHINGTON 7, D.C.

# A THEORETICAL AND EXPERIMENTAL STUDY OF PROPELLER-SHAFT FAILURES

by

Norman H. Jasper

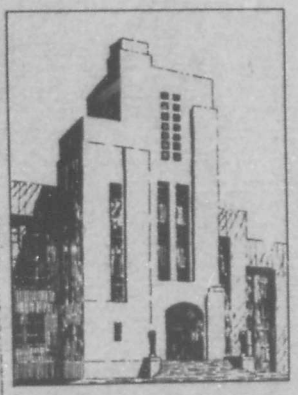







August 1953

Second Printing

Report 808

NS 712-038

First Printing - July 1952

TABLE OF CONTENTS


T-2 TANKER, MISSION SAN LUIS OBISPO

# A THEORETICAL AND EXPERIMENTAL STUDY OF PROPELLER-SHAFT FAILURES

by

Norman H. Jasper

**ABSTRACT**

**This report presents a detailed study of the stresses in the tailshaft of a T2-SE-A2 tanker of the MISSION type, including an analysis of the causes of tailshaft failures encountered in these ships as well as in Liberty ships and other ships of similar type. The study, conducted on behalf of the U.S. Navy and the Society of Naval Architects and Marine Engineers, is based on full-scale tests as well as on theoretical analyses. Special emphasis is placed on the effects of a whirling type of flexural vibration on the stresses and motions of the shaft. Design methods are evaluated in the light of the above analysis.**

**One of the principal conclusions is that the shaft failures are due to a lack of endurance strength of the shaft as designed and built and not due to a serious lack of endurance strength of the shafting material itself. This lack of endurance strength appears to be associated with the microscopic stress variations rather than with macroscopic stress variations.**

## 1. INTRODUCTION

A study of the lateral vibration of propeller shafts was authorized by the Bureau of Ships[1,2] as a direct result of the numerous fractures of propeller tailshafts on single-screw vessels of the Liberty, the T2-SE-A2 tanker, and similar types (Maritime Commission designs C-1, EC2, and C-4). Owing to the importance of the problem, the Society of Naval Architects and Marine Engineers appointed a panel to study it and, if possible, to make recommendations for alleviation of the situation. The Navy program, of which this investigation is a part, will be coordinated with the work of the Society of Naval Architects and Marine Engineers.

Tailshaft failures have received considerable attention in the last several years; see, for example, the papers published by S. Archer[3] and A.R. Gatewood.[4] To get an idea of the extent of these failures the following is quoted from Reference 3.

---

[1]References are listed on page 64.

> "The construction of the largely welded dry cargo "Liberty" type of vessel was begun in the United States in January 1942, and altogether no less than 2580 were built, of which 2315 remained at the conclusion of hostilities, representing a total gross tonnage of nearly 17 million tons, or about 20 percent of the world total for 1947 of all vessels greater than 500 tons gross. Information at 1 December 1948 revealed that altogether a total of 583 "Liberty" screw-shafts have been renewed, including during the past three years about 100 casualties at sea with resulting loss of propeller. The cost of these breakdowns in salvage and demurrage charges alone needs no emphasis."

From the Navy's standpoint, the high incidence of shaft failure (as nigh as 50 percent in some classes) threatens to create a serious bottleneck in the nation's drydock and ship repair facilities in a time of great shipyard activity.

A number of theories have been proposed to account for the high incidence of cracked tailshafts. One of these[5] suggested that the primary cause of the failures was a resonant whirling vibration of the shaft at propeller blade frequency (rpm × number of propeller blades). Inasmuch as the design of such shafting has been based primarily on the transmitted torque and the deadweight transverse loads, and since the appearance of many shaft failures indicated that bending stresses are significant, it was thought advisable to consider the several contributary factors that might induce bending stresses.

It was decided therefore that the David Taylor Model Basin would conduct an analytical and experimental investigation of the lateral vibration of propeller-shaft systems on behalf of the Bureau of Ships and the Society of Naval Architects and Marine Engineers. The investigation presented here is a detailed study of the stresses in the tailshaft of a T2-SE-A2 tanker of the MISSION type (10,000 hp), including an analysis of the causes of the shaft failures occurring on these ships. A T-2 tanker was selected for the full-scale sea tests because (a) it was a type which had experienced shaft failures, (b) a number of these ships were owned by the U.S. Navy, (c) a ship could be made available, and (d) extreme conditions of trim could readily be obtained by water ballasting. The prime objective of this test was to determine the magnitude and nature of the stresses* in the tailshaft under actual operating conditions.

---

*In order to avoid misunderstanding later it shall be understood that whenever the term "measured stress" is used in this report it denotes a stress calculated on the basis of measured strains.

This report will first present some background information on the flexural vibration of shafting. Next, the over-all problem is analyzed in order to determine the most suitable approach to its solution. The full-scale test program is then set forth and the test results are presented and analyzed. Conclusions and recommendations are given at the end of the report.

The appendix presents a rough analysis of the vibration data obtained by the General Electric Company for the Society of Naval Architects and Marine Engineers during these T-2 tanker tests. The Taylor Model Basin did not participate in planning the test made by General Electric; the material in the appendix is given in this report primarily for the sake of completeness.

## 2. BACKGROUND DISCUSSION

The subject of lateral vibration of propeller-shafting systems has been brought into focus by the great number of propeller-shaft failures on single-screw vessels and has also received some attention in connection with the vibration of the tailshafts of destroyers and similar ships.[6,7] On destroyers the problem was one of excessive vibration. On the T-2 tankers and Liberty ships it was not known whether or not the excessive strains were, in fact, associated with excessive lateral vibration; if they were, the character of the vibration was unknown.

A paper by E. Panagopulos[5] in which it was suggested that the shaft fractures were due to a fourth-order resonant whirling vibration has received rather wide attention in naval and marine circles. Mr. Panagopulos' contention was based on a model experiment made by him and on his calculations of the natural frequencies of lateral vibration of the shaft propeller systems for those classes of ships which have been subject to shaft failures. In a discussion of this paper[8] it was indicated that a calculation of the natural frequency of such systems was, by its nature, of doubtful value and that there existed a definite possibility that the excessive shaft stresses were due to excessive external loads on the propeller, aside from resonance effects.

It would be of great value if it were possible to calculate the natural frequency of whirling vibration of propeller-shafting systems. An exact analytical treatment of the problem is impractical even if one considers only the solution of the applicable differential equations. But apart from mathematical difficulties there are many more difficulties due to the lack of knowledge of the boundary conditions, as for example, the stiffness and position of the bearing restraints. It is not the intention here to go into an extensive analytical treatment of shaft vibration—that will be done in a future TMB report—but it is of value to indicate the difficulties and the approach that would appear to promise usable results.

Two general methods appear to be practical; one might be called the experimental approach and the other the pseudo-analytical approach. In either method the physical parameters of the system will have to be determined by some means. The actual and the predicted values of natural frequency may then be correlated by means of some empirical "factors of ignorance." In one type of approach, a physical, electrical, or other model of the system is built; its natural frequencies are determined by test, and from these values the prototype characteristics are calculated. In one pseudo-analytical approach the natural frequency of a shaft is calculated in a simplified manner, omitting the effects of the propeller, and then the frequency of a massless shaft carrying the propeller, etc., is calculated, and the separate effects are combined by means of Dunkerly's formula[9] to obtain an approximation to the fundamental natural frequency of the actual system.

For the purpose of the discussion to follow, whirling will be regarded as the resultant of two linear flexural motions of the shaft in two planes at right angles to each other. If the frequency of these two vibrations is the same, then the center of the shaft will move in an elliptical path which, under special conditions, may take the form of circular or straight-line motion. First-order whirling of propulsion shafting, with a frequency equal to the frequency of rotation, is a common and well-known occurrence. It is caused by an unbalanced shaft-propeller system. According to Timosnenko[10] whirling vibrations may also be excited by hysteresis of the shafting material. It is the higher-order whirls that are of special interest here, especially from the standpoint of their excitation.

A simple shaft-propeller system will be discussed in order to indicate the possibility of whirling motions in the absence of gyroscopic effects and to study the stress variation at a point on the shaft for various assumed types of whirl. If the propeller is considered as a rigid rotor, it will be shown that a whirling of its center about the shaft axis may be produced at any frequency due to variations in external moment of the hydrodynamic forces. It can also be shown that resonant whirling motions can exist at certain natural frequencies, and that gyroscopic effects are significant in a determination of these natural frequencies. A higher-order whirling motion could, of course, also be excited directly by externally applied moments such as are generated by higher-order wake components, even though gyroscopic effects be negligible.

The resultant of the pressure acting on the elements of all the blades is a force which, in general, has a variable magnitude, direction, and point of application, that is, all these quantities may continually change as the propeller rotates. The pattern of the variation repeats periodically,

with a period equal to the time required for one shaft revolution divided by the number of blades. The bending moment acting at any given shaft section may be represented by a vector, the length of which (that is, its numerical value) varies with time and which rotates at some multiple of the propeller speed. The stress at any point on the shaft can be expressed by the familiar beam formula

$$\text{Stress} = \frac{Mc}{I}$$

where M is the effective bending moment at the shaft section under consideration and c is, as usual, the distance from the neutral axis in bending to the point considered. It should be noted that the shaft may be rotating at a different speed and in a different direction than the moment vector, and therefore c will be a function of time. In practice, the effect of resonance and gyroscopic effects may be important. The resonance effects can be taken account of by calculating an effective bending moment. The most indeterminate quantity required for a stress calculation is the bending moment variation. This variation can be computed from the propeller design and the wake diagram; such a computation has been carried out for the T-2 tanker and will be discussed later. The severity of the higher-order whirling motions and strains varies as the magnitude of the higher-order components of the moment variation.

A mathematical expression for the stress variation at a point P due to an effective, statically applied, bending moment M will now be derived (see Figure 1). Let

- $\xi$ be a phase angle locating the point P relative to the reference position (in which a propeller blade is pointed in the direction of the Y-axis at time t = 0),
- $\omega t$ the angle of shaft rotation from t = 0,
- $\phi$ the whirling angle,
- n the order of moment variation (referred to shaft rpm),
- c the distance of point P' from the neutral axis,
- R the maximum value of c, and
- I the moment of inertia of the shaft in bending.

Let P be the position of any point on the shaft at the instant t = 0, and P' be the position of the same point at some later time t. Then

$$c = R \sin\left[\left(\frac{\pi}{2} + \phi\right) - (\omega t - \xi)\right] = R\left[\sin(\omega t - \xi)\sin\phi + \cos(\omega t - \xi)\cos\phi\right]$$

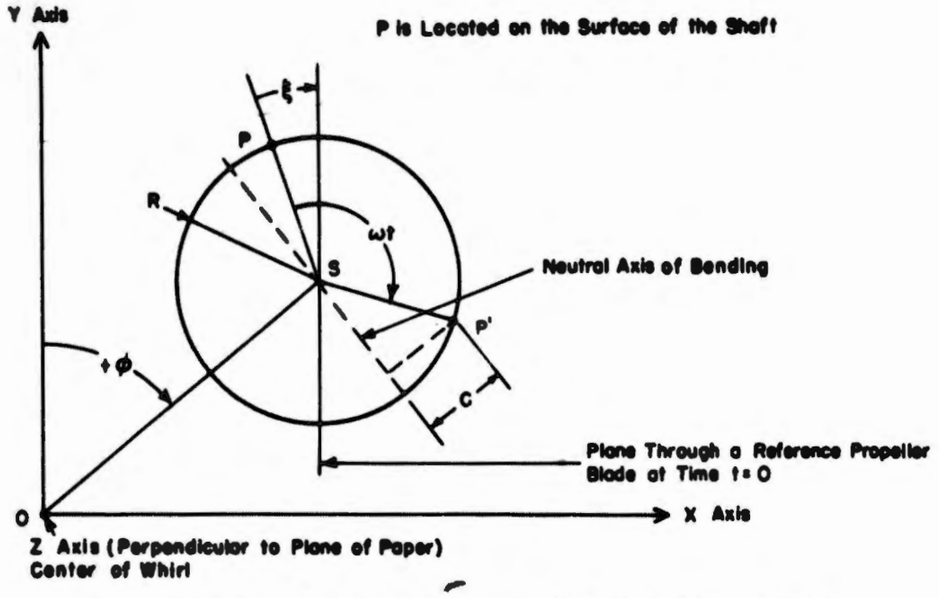


Figure 1 - Section Through the Whirling Shaft

The whirling motions considered here are restricted to the type in which the axis of the shaft lies in a plane which contains the radius OS and the Z-axis (curvature in one plane only).

If the bending moment in the YZ-plane is denoted by $M_y$ and that in the XZ-plane by $M_x$, then the resulting moment may be represented by the vector $\vec{M}$. The magnitude of $\vec{M}$ is $|\vec{M}|$, and its angular position is $\phi$ which will be called the whirling angle.

$$|\vec{M}| = \left(M_x^2 + M_y^2\right)^{1/2}$$

$$\phi = \text{arc tan}\frac{M_x}{M_y}$$

The bending stress due to the application of the bending moment $\vec{M}$ is

$$\text{Stress} = \frac{|\vec{M}|}{I}c = \frac{|\vec{M}|}{I}R\left\{\sin(\omega t - \xi)\sin\phi + \cos(\omega t - \xi)\cos\phi\right\}$$

These formulas will be applied to some typical illustrative cases.

Case A: Assume that a whirl of n times the shaft speed exists. Then, for $\xi = 0$, $\phi = n\omega t$,

$$\text{Stress} = \frac{M}{I}R\cos(n - 1)\omega t$$

when the whirl and shaft rotation are assumed to have the same direction, and

$$\text{Stress} = \frac{M}{I} R \cos(n + 1)\omega t$$

when the whirl and shaft rotation are assumed to have opposite directions.

Case B: Assume the bending moment $M_x$ is zero, and $M_y = M_{y_0} \sin n\omega t$. Then, for $\xi = 0$, $\phi = 0$,

$$\text{Stress} = \frac{M_{y_0}}{I} R \sin n\omega t \cos\omega t$$

Case C: Assume that $M_x = M_R \cos n\omega t$, $M_y = M_R \sin n\omega t$, $\xi = 0$, and $\phi = n\omega t$. Then $|\vec{M}| = M_R$ and

$$\text{Stress} = \frac{M_R}{I} R \cos(n - 1)\omega t$$

In this case, which is seen to be identical to Case A, the shaft has a circular whirl of n times the propeller rpm, and the strain variation consists of n-1 cycles of strain per shaft revolution. It is assumed that the rigidity of the shafting system is the same in all planes through the shaft.

It should be noted that, if the propeller is not completely immersed in water during operation, it will be subjected to an applied bending moment which does have components in both the vertical and horizontal planes and can therefore be expected to cause simultaneous deflections in these two planes. From the preceding discussion it is evident that a whirling motion may be caused by (1) a combination of an applied bending moment together with the gyroscopic effect of the spinning propeller and (2) by the applied bending moments alone if these moments have components in more than one plane. A mathematical treatment of gyroscopic effects will be given in a forthcoming TMB report.[11] In either case, resonant vibrations may be present and cause severe stresses.

## 3. ANALYSIS OF THE PROBLEM

Some classes of single-screw vessels equipped with four-bladed propellers, such as the T-2, C-2, C-4, and Liberty Maritime Commission designs, have been experiencing an extremely high rate of tailshaft fractures even though the design and construction of the shafts and propellers has followed accepted practice. The appearance of the fractures shows that they are caused by combined torsion and bending stresses and that progressive fracture has

taken place (fatigue failure). Bending failures predominated in all vessels except in the Liberty ships.

The discussion of the preceding section indicates that these failures may be due to the resonance effects of vibratory motions, to excessive applied loads, or to a combination of both. Remedial measures would vary depending on which factors predominate. The following questions arise:

A. What are the magnitudes of the actual stresses in the tailshaft near the location of the failures?

B. Does the magnitude or the character of the stresses vary appreciably with the draft and trim of the ship, and if so, why?

C. What is the character of any "stress concentration" present and how serious are its effects?

D. Is the contention of Mr. Panagopulos, that a fourth-order whirling resonance is present near the operating rpm of these vessels, valid?

E. Are the stresses caused primarily by excessive external forces or by resonant vibrations?

F. What are the magnitudes of the external forces acting on the system?

G. What are the fundamental natural frequencies of flexural vibration of the propeller-tailshaft system? What is the effect of the surrounding water water on these frequencies?

H. Is it possible to determine the natural frequencies of lateral vibration, on the basis of ship's plans, with a reasonable degree of accuracy?

The only way in which most of these questions can be at least partially answered is by actual tests on a vessel. To get the information required under Items A and B it is necessary to measure the strains in the tailshaft just forward of the propeller hub for several conditions of speed and loading. In making such measurements it will be advisable to plan them in a manner which will provide data free of stress-concentration effects. The latter effects may be studied separately by means of models, photoelasticity, examination of failures, and analytical analysis. The magnitude of the external forces may be estimated from a knowledge of the stresses and of the shaft rigidity.

The relative significance of resonance effects, as well as the character of the vibratory effects, can be determined from strain data obtained at a number of shaft speeds and for a number of ships' maneuvers. It has been shown, Section 2, that the frequency of the strain variations is $(n \pm 1)$ times the shaft rpm, when n is the order of the whirling motion. Therefore, the

strain-time oscillograms will indicate the order of whirls that do exist. The natural frequency of vibration of the propeller-shafting system may be excited by means of a vibration generator, with the propeller both in and out of the water. The frequencies thus determined may then be checked against the values calculated by various means.

It is evident that the most direct and promising approach to a solution of the problem requires the measurement of strains in the tailshaft under various normal operating conditions and under occasional overload conditions.

The type of shaft failures experienced so far has indicated that, in the case of geared turbine and electric drives (T-2, C-2, C-4, Victories) bending stresses predominate, whereas the steam-engine-equipped Liberty ships evidence combined torsion-bending failures. It was decided to conduct the tests on a T-2 tanker as its trim could conveniently be changed by liquid ballasting and a vessel was readily available. It was desired to complete the tests as rapidly as possible after completion of the strain-gage installation in order to decrease the possibility of gage failures.

## 4. TEST PROGRAM AND TEST INSTALLATION

### 4.1. TEST PROGRAM

The tests can be divided into two logical groups: First, those with the ship in dock to determine the natural frequencies of the propeller-shaft system, and second, those at sea to determine the actual stresses under operating conditions.

#### 4.1.1. Vibration Generator Tests in Drydock

A. The ship was docked; the existing tailshaft was replaced with a special test shaft modified in accordance with Figure 2; and a vibration generator was installed on the propeller.

B. Vibration-generator tests were conducted with the ship in drydock, to determine the natural frequencies of flexural vibration of the shaft-propeller system (nonrotating shaft).

C. The vibration-generator tests were repeated with the vessel waterborne, to determine the effect of the virtual mass of water.

D. Upon completion of Items A, B, and C all test gear was removed.

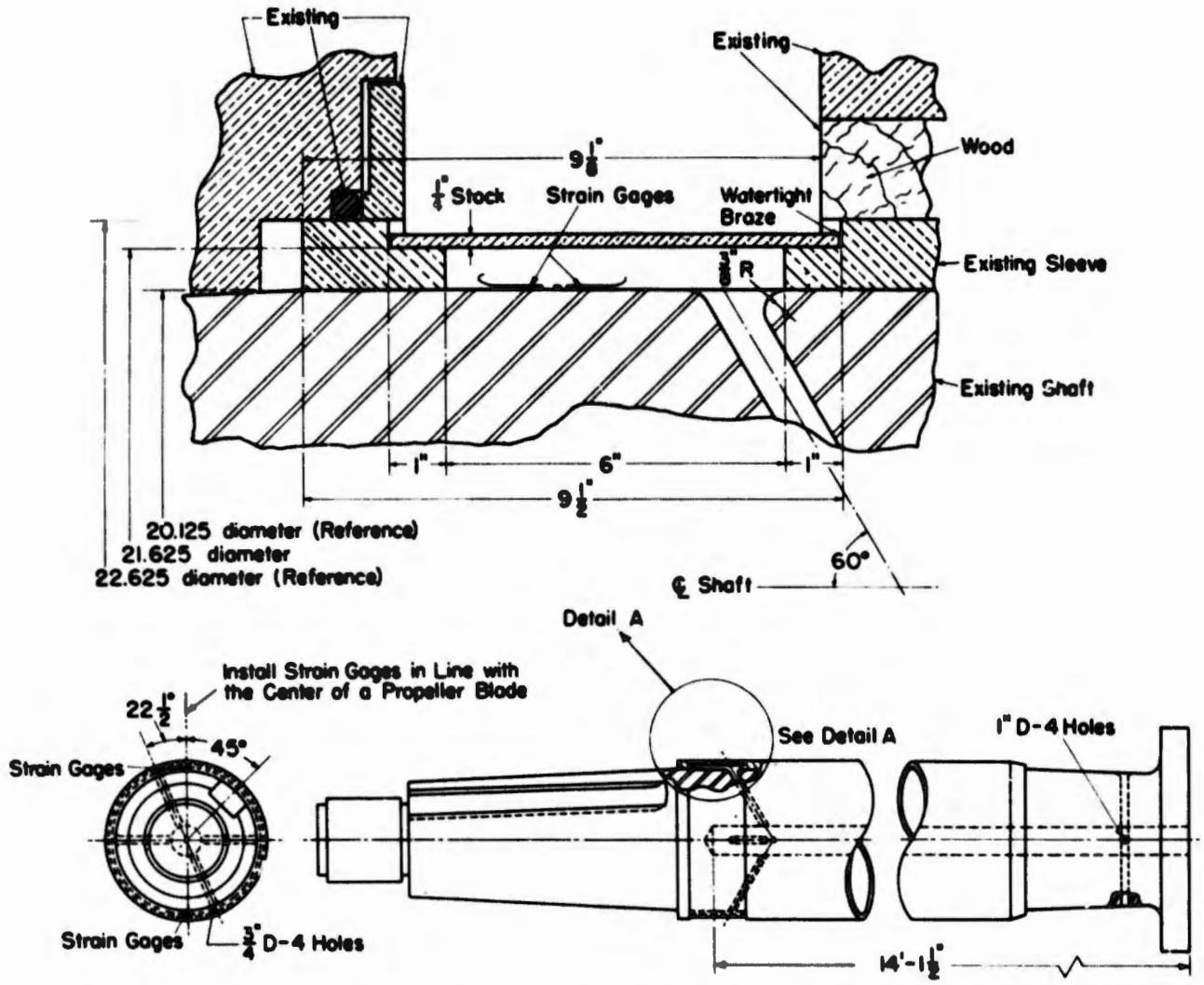


Figure 2 - Modifications of T-2 Tanker Tailshaft

4.1.2. Underway Tests at Sea

The torsional, bending, and axial strains in the tailshaft just forward of the propeller hub were measured and, in addition, measurements were made of the torsional and translational vibration of the tailshaft as well as the linear vibratory motion of the hull near the fantail for each of the following test conditions.

A. With the ship on a straight course, the speed was varied continuously from zero to full-power shaft rpm.

B. With the ship on a straight course, the speed was varied from 45 rpm to full-power rpm in 5-rpm intervals.

C. With the ship proceeding at full power on a straight course, the order "rudder hard over" was executed as rapidly as practicable.

D. If critical shaft speeds were noted, measurements were to be made at such speeds, both on a straight course and during a hard turn.

These tests were to be conducted both with the vessel in the full-load condition and in a light-ballast condition trimmed so that the propeller is only partially immersed.

## 4.2. INSTRUMENTATION INSTALLATIONS

### 4.2.1. Strain Gages

The solid tailshaft was modified as shown in Figure 2 in order to permit a watertight installation of SR-4 strain gages and to allow the cables to be run from the strain gages to the slip-ring assembly which was located on the first line-shaft sections. A set of active and temperature-compensating gages were connected in the form of a bridge circuit for each type of strain measurement; see Figure 3. The bridge was excited by a 2200-cps oscillator. Both excitation and signal voltages were transmitted via a set of slip rings and brushes to the amplifying and recording equipment. The strain gages were installed at a position about 22.9 inches forward of the center of the propeller, and longitudinal strain gages were placed in line with the center of a propeller blade.

A variation in contact resistance exists between the brushes and the slip rings. This variation will give rise to undesirable voltage variations whenever current is flowing through the contacts, and the magnitude of the voltage variation will be proportional to the current. By careful initial balancing of the strain-gage bridge with the shaft at rest, on the gage side of the brushes, circulating unbalance currents due to a static unbalance of the bridge are minimized, thereby minimizing the voltage variation due to variable brush contact resistance (brush noise).

The amplifiers were TMB Type 1B strain indicators, and the strain signals were recorded on a 14-channel Consolidated oscillograph equipped with 4-ma string galvanometers. The strain gages themselves were waterproofed by first coating the properly prepared gages with "Insulex" varnish and then filling the annular space around the shaft, containing the gages, with "Tuffernel," a Westinghouse plastic which is applied in liquid form and is cold setting. The gages were installed so as to be relatively unaffected by stress concentration (about 22.9 inches forward of the center of the propeller hub).

The tailshaft is shown in Figure 4, which also shows one of the wrapper plates that were installed to protect the gages. The strain-gage installation is shown in Figure 5, and Figure 6 shows the slip ring and brush installation on the line shaft. The amplifying and recording equipment is shown in Figure 7.

It is of interest to note that the ship's tailshaft, which was replaced by the instrumented experimental tailshaft, did evidence cracks under magnaflux examination.

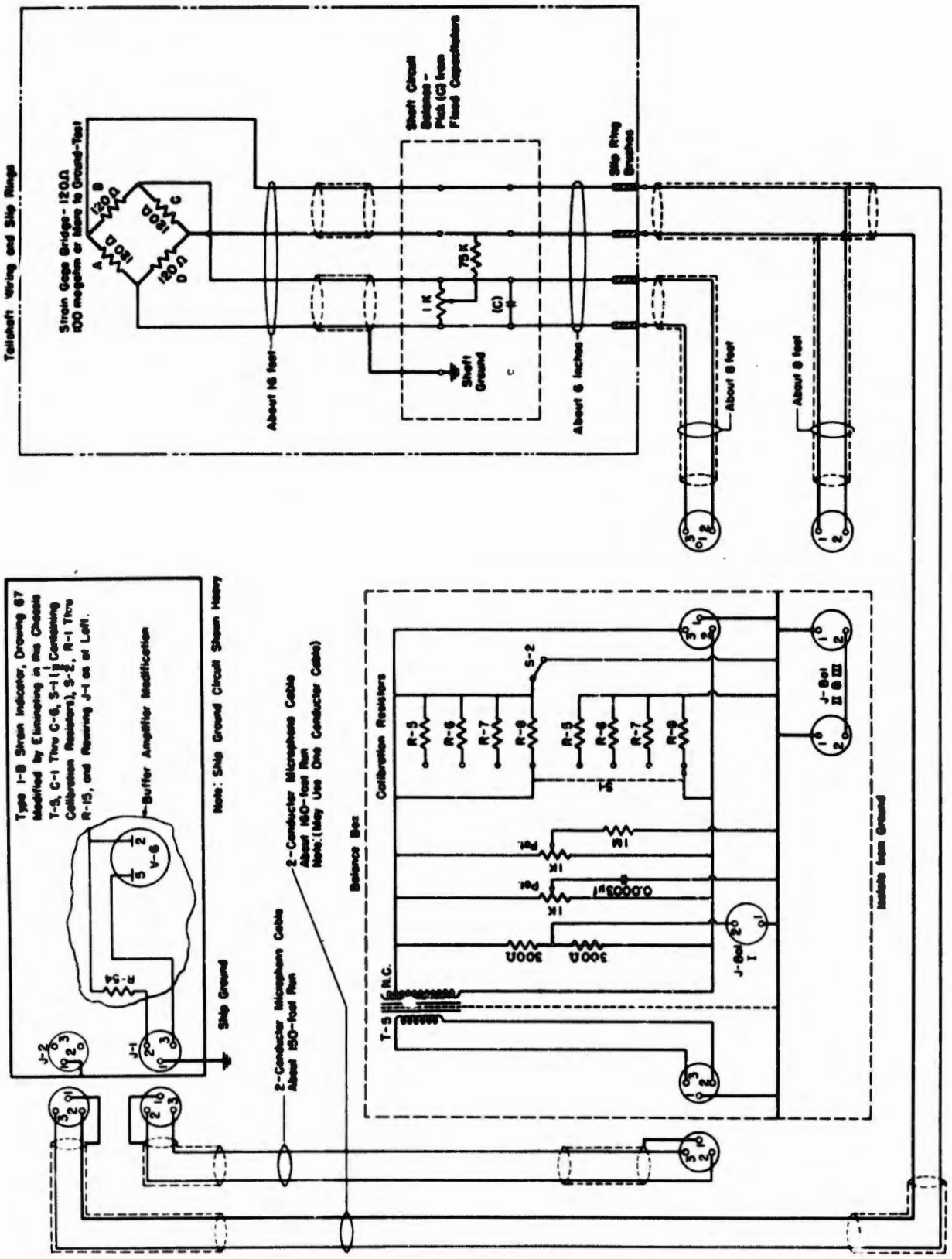


Figure 3 - Schematic Wiring Diagram of Strain Gage Installation for Propeller Shaft of T-2 Tanker

Slip rings made of naval gun metal bronze. Brushes made of 65 percent silver and 35 percent graphite.

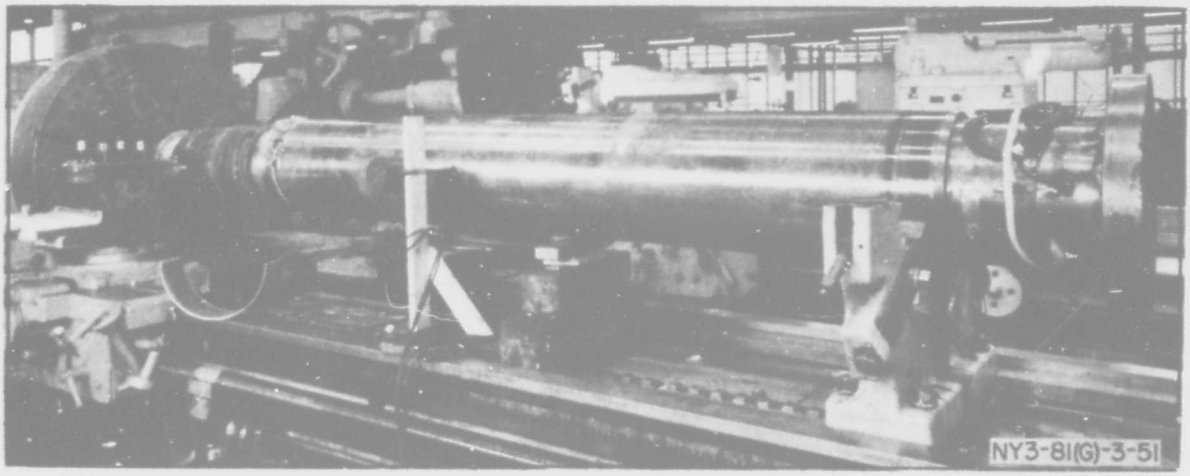


Figure 4 - Photograph of Experimental Tailshaft

4.2.2. Vibration Pickups

The General Electric Company installed several G.E. electromagnetic pickups in order to measure the lateral motions of the tailshaft. Four pickups were installed at the outboard end of the stern tube bearing (see Figure 8) to measure the vertical and horizontal components of shaft motion. Similar measurements were made at the first steady bearing. The output of these gages was recorded on a string oscillograph.

In order to measure the hull vibration, two vacuum-tube accelerometers, built by the Calidyne Company, were installed on the fantail; their output was recorded, together with the strain data, on a single Consolidated oscillograph. In addition, TMB direct-recording pallographs were installed at the location of one of the vacuum-tube accelerometers. Measurements of the torsional vibration of the propeller shaft were made by the Material Laboratory, New York Naval Shipyard,[12] by means of a Geiger oscillograph, which had been located 19 feet 6 inches forward of the stuffing-box bulkhead.

4.2.3. Instrumentation for the Vibration Generator Test

A Lazan vibration generator[13] was installed on the hub of the propeller to permit excitation of flexural shaft vibration in both the vertical and horizontal planes for either the dry or submerged condition. The vibratory motion of the propeller and shafting was measured with both Calidyne vacuum-tube accelerometers and with a Shure crystal accelerometer working into a General Radio meter; the output of the General Radio meter was again amplified by a Brush amplifier and recorded by a direct-inking Brush oscillograph.

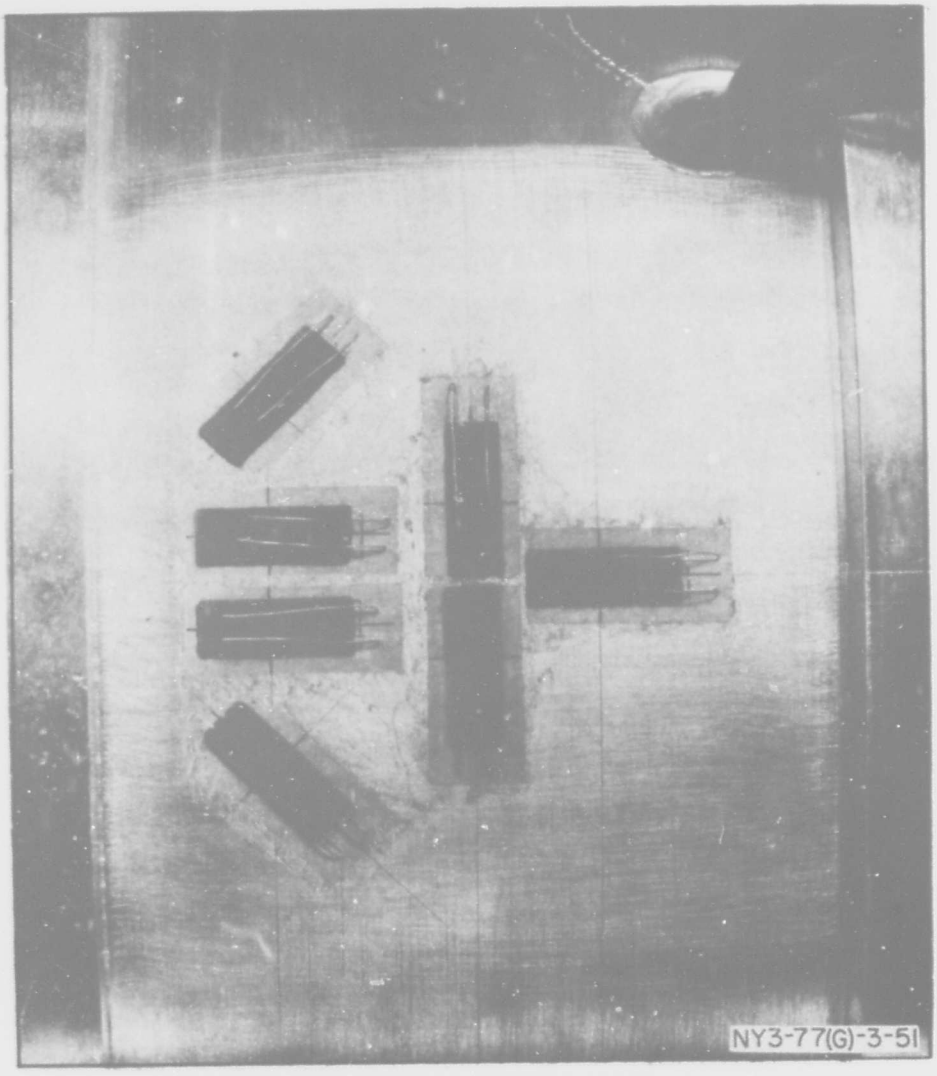


Figure 5a - Close-Up of Gages

The output of the Calidyne pickups was amplified and recorded by a Consolidated oscillograph.

A sketch and photograph showing the waterproof installation of the vibration generator are shown in Figures 9 and 10 respectively.

## 5. TESTS AND TEST RESULTS

### 5.1. VIBRATION GENERATOR TESTS

The Lazan vibration generator was installed in its watertight housing (Figure 9), and this assembly was then firmly attached to the propeller hub (Figure 10). The frequency of force application was varied continuously from zero to about 1200 cpm, and the response of the propeller was measured

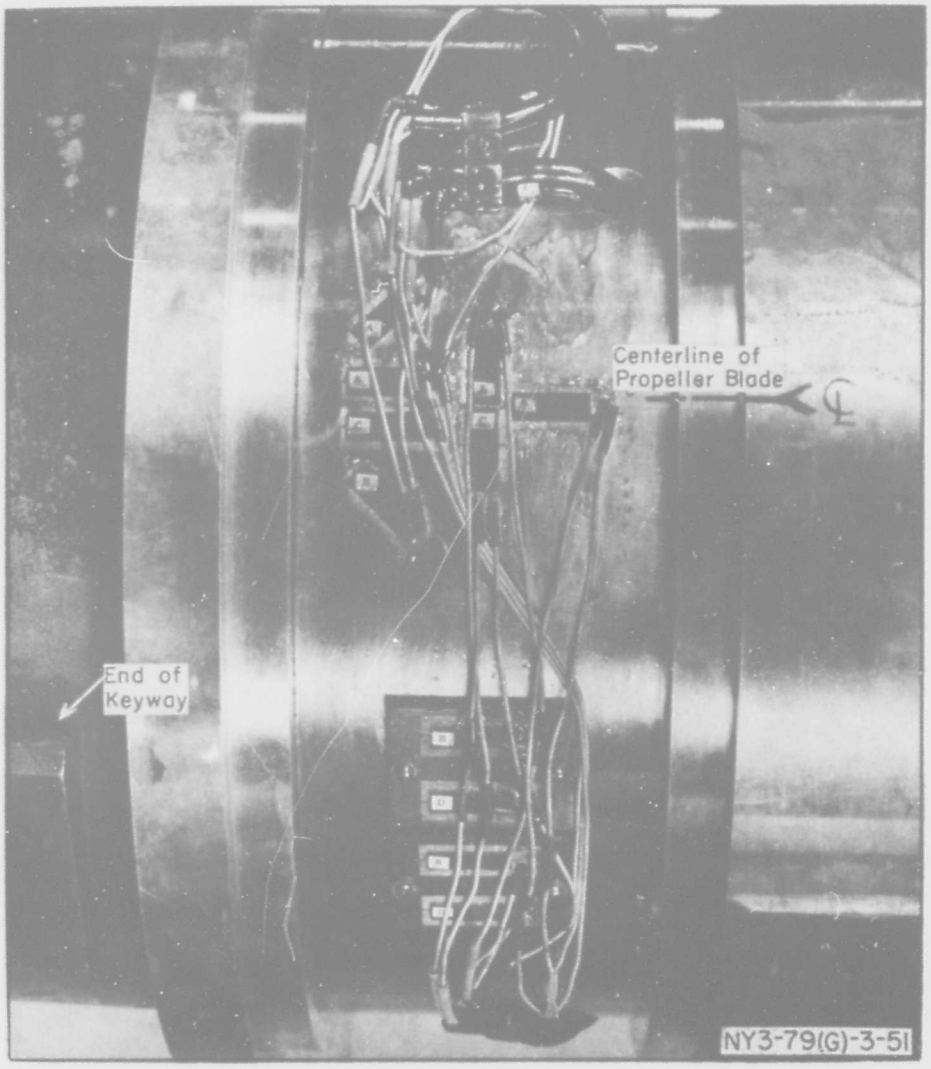


Figure 5b

Figure 5 - Photographs of Strain Gage Installations

by means of vibration pickups. This procedure was followed to determine the natural frequencies in both the vertical and horizontal planes. A check was made to determine the relative amplitudes and phase relationships between the motion of several points on the propeller and tailshaft in order to ascertain that the measured resonance was a resonance of the entire system. The natural frequencies were determined with the shaft-propeller system in air and with the system submerged in water.

Graphs of the relative amplitude of vibration plotted on a basis of frequency are shown in Figure 11. It is quite apparent that the resonances of the system are different in the horizontal and vertical planes. A sample oscillogram of the measured vibration is given in Figure 12.

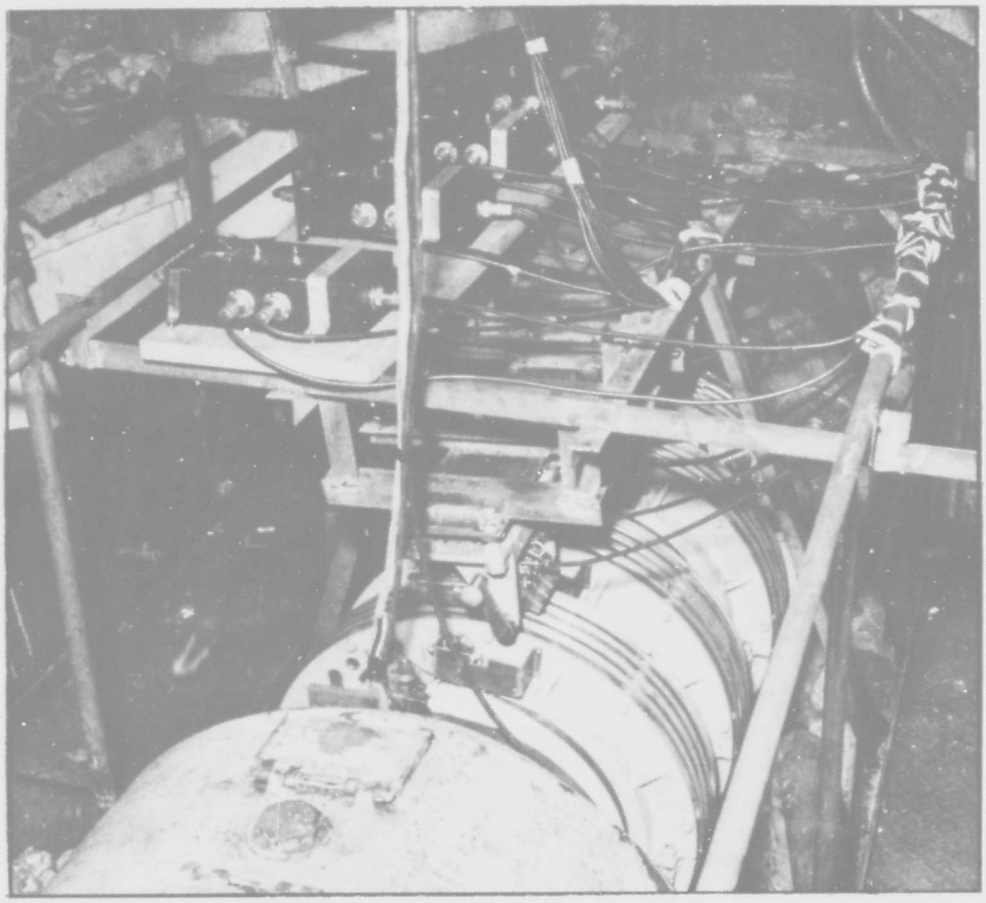

Figure 6 - Photograph of Slip Ring and Brush Installation on Tailshaft

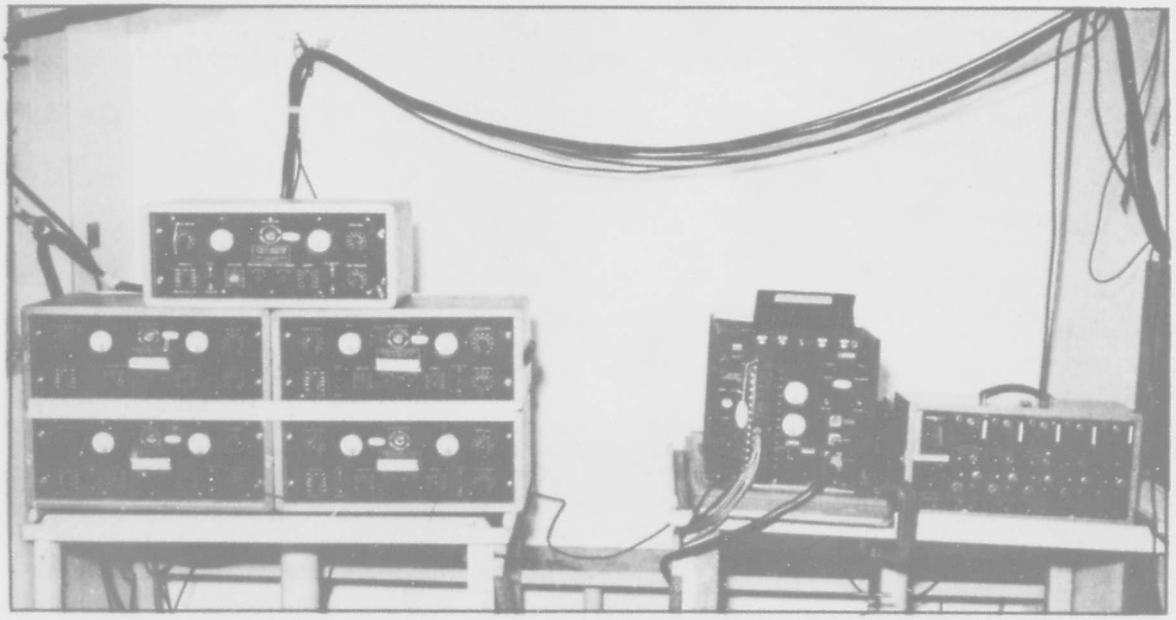

Figure 7 - Photograph of Amplifying and Recording Equipment
Used on T-2 Tanker Test

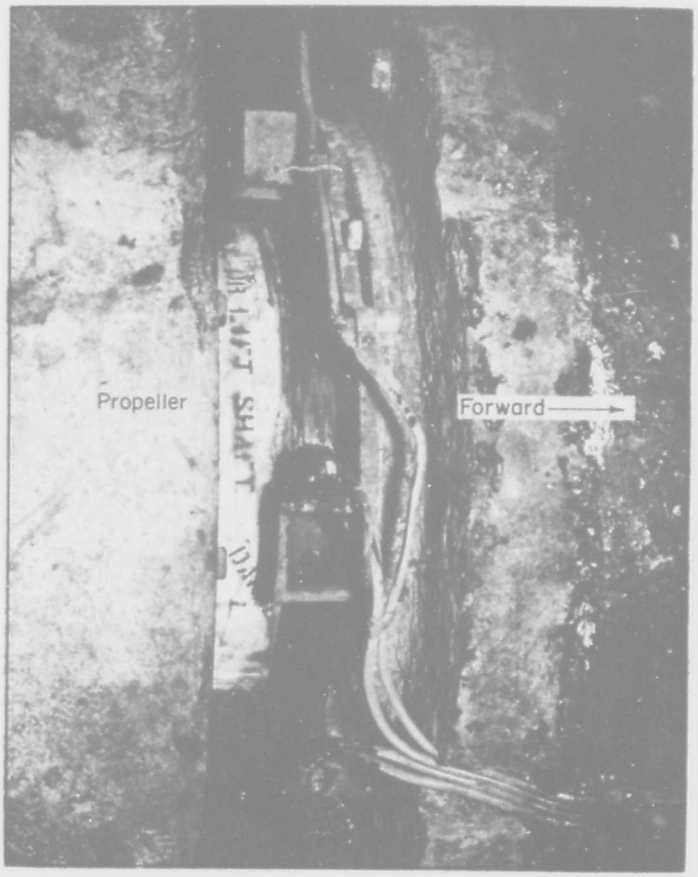


Figure 8 - Installation of General Electric Company Displacement Pickups at After Stern Tube Bearing

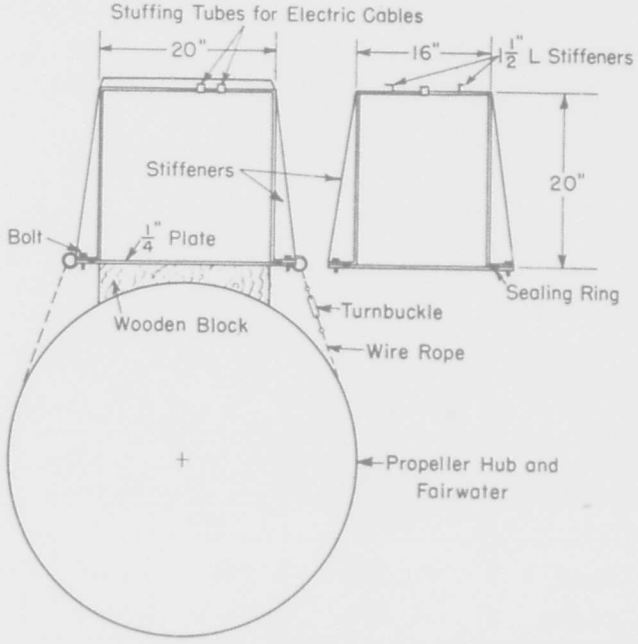


Figure 9 - Watertight Installation of Lazan Vibration Generator

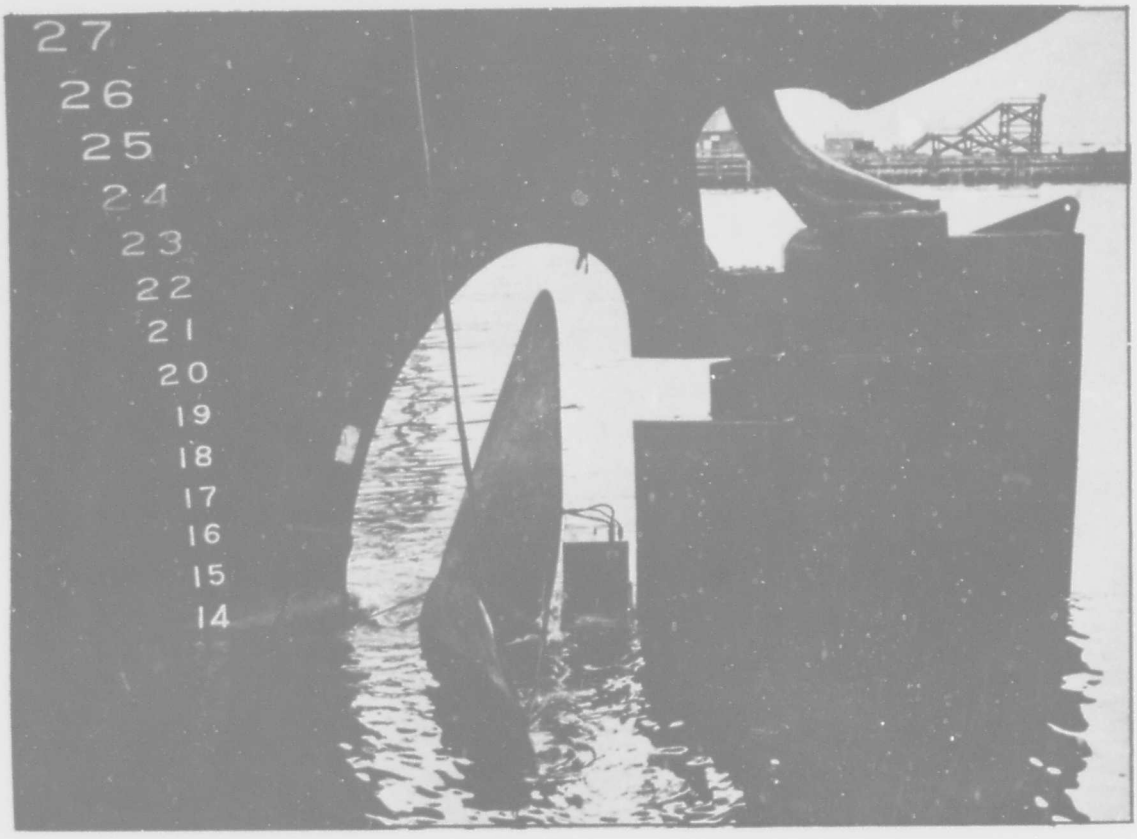


Figure 10 - Watertight Installation of Vibration Generator on Propeller Hub of T-2 Tanker

5.2. UNDERWAY TESTS

The ship was operated with two conditions of loading; see Table 1. For each of the two conditions the vessel was run through the schedule of tests listed in Section 4.1.2. except that the continuous run, Item A, was omitted for the load condition and that a crash back was made from full-power

TABLE 1

Test Conditions of T-2 Tanker

| Condition | Displacement tons | Draft, ft-in. | | |
|---|---|---|---|---|
| | | Forward | Aft | ⌀ |
| Load | 20,300 | 28-0 | 28-6 | 28-3 |
| Light | 9,270 | 14-0 | 14-0 | 14-0 |

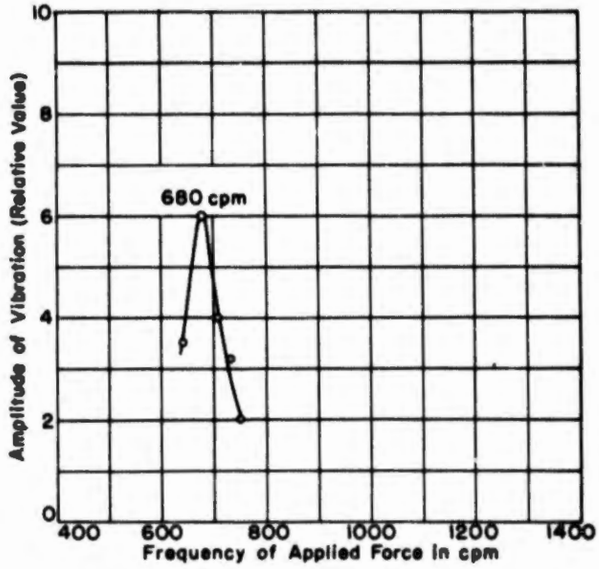


Figure 11a - Horizontal Excitation of Shaft

Propeller shaft system immersed in water.

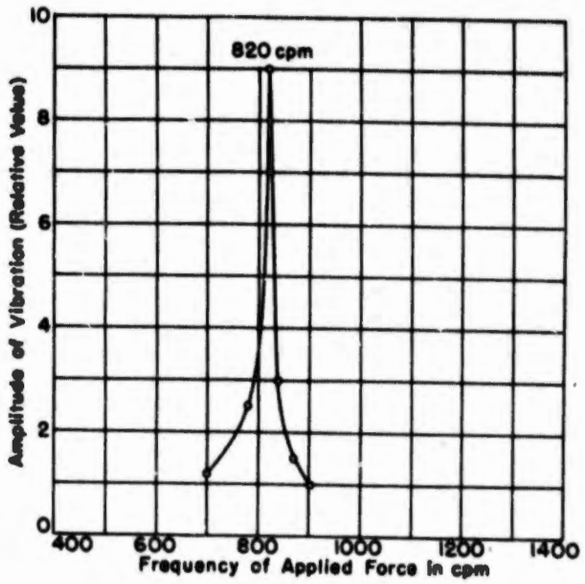


Figure 11b - Vertical Excitation of Shaft

Propeller shaft system immersed in water.

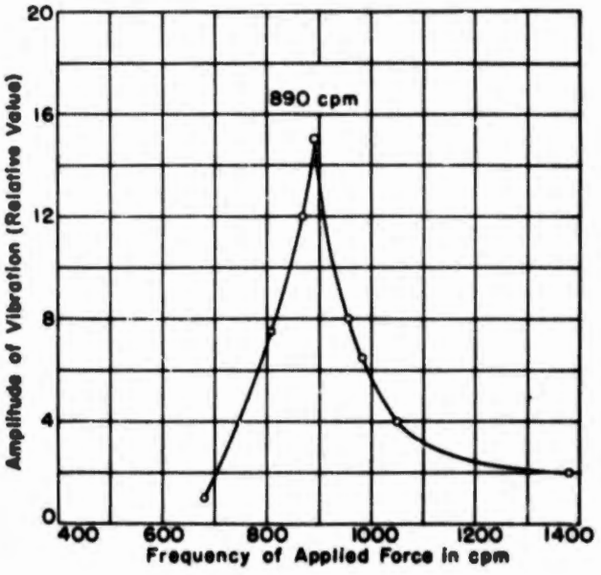


Figure 11c - Horizontal Excitation of Shaft

Propeller shaft system in air.

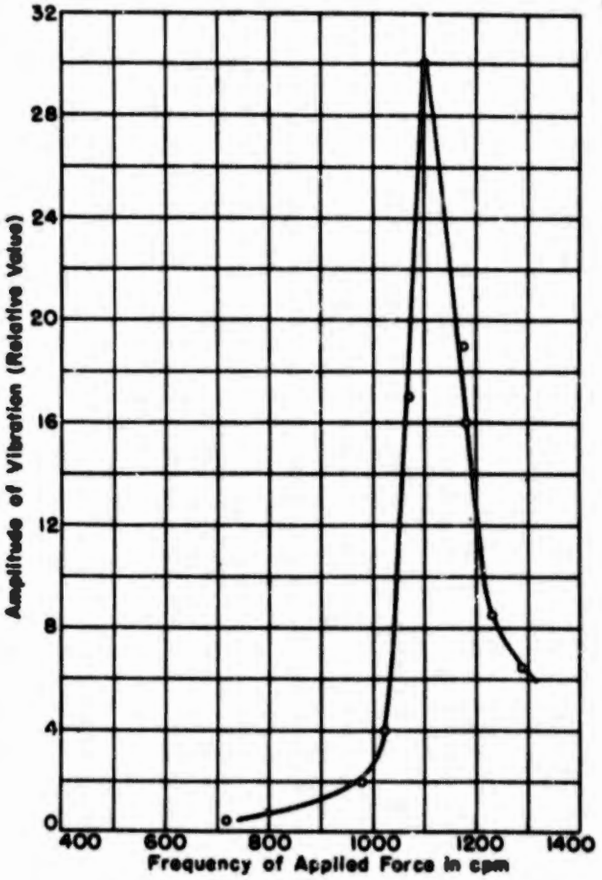


Figure 11d - Vertical Excitation of Shaft

Propeller shaft system in air.

Figure 11 - Resonance Curves of Propeller-Shaft System

The system was excited by a force which varied as the square of the frequency of excitation.

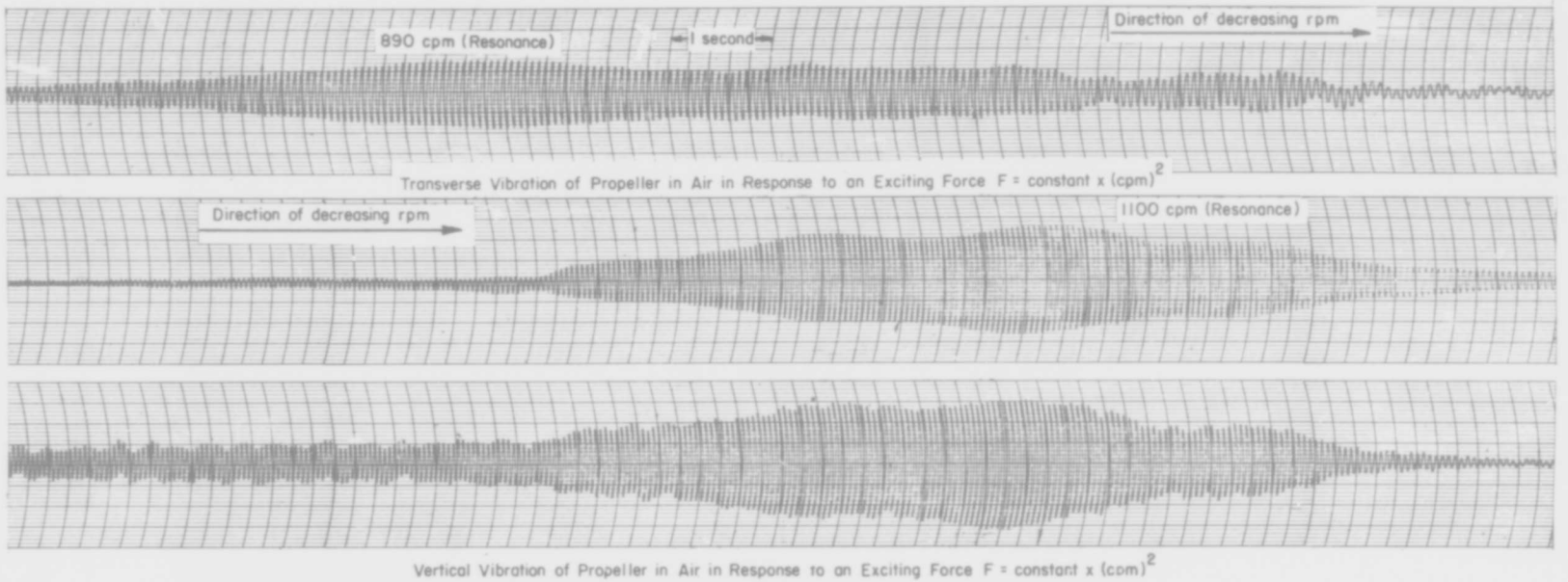


Figure 12 - Sample Oscillogram Obtained During Vibration Generator Test of Propeller-Shaft System

ahead to full-power astern at the end of the load-condition tests. Strains were measured during each of these runs; sample oscillograms showing the strain gage signal, are shown in Figure 13. Strains were also measured on several occasions during the tests, while the shaft was slowly turned over with the jacking gear; the bending strains measured during this operation are due to the action of gravity and buoyancy alone and therefore will permit separation of these effects from the total measured strains.

The hull vibration (Figure 14) was quite small during the underway tests; even during hard turns and crash-back operations only relatively small amplitudes were observed. The magnitude of the first-order (shaft rpm) vibration was negligible. Evaluation of the Geiger torsiograms showed that the amplitude of torsional vibration at the point of measurement (19 feet 9 inches forward of the stuffing box) was small, never exceeding $\pm 0.1$ degree. The vibration was of the fourth order referred to the shaft rpm. Owing to the low magnitude of the torsional-vibration signal, it was not possible to evaluate the amplitudes of vibration accurately and determine the location of critical speeds on the basis of vibration measurements. It will be shown later that the presence of a torsional resonance was established on the basis of the torsional strain data.

## 6. ANALYSIS OF RESULTS

### 6.1. FLEXURAL VIBRATIONS OF PROPELLER SHAFT SYSTEMS

Before attempting to analyze the strain variations it will be well to consider first the flexural, especially the whirling motions of the shaft.

It was stated in Section 2 that the accurate analytic determination of the natural frequencies of flexural vibration of a ship's propeller-shafting system was impractical because (a) the lack of knowledge as to the effective physical constants of the system and (b) the mathematical difficulties involved. The mathematical difficulties can be partially circumvented by utilization of mechanical and electrical models.

First, an electrical analog has been used to show the effect of variations in the location of the aftermost bearing support on the natural flexural vibration frequency of the T-2 tanker shaft system. The difference equations for the system can be derived from the differential equations governing the motion of the propeller. A passive electrical circuit having analogous difference equations is set up and the resonance frequencies of the electrical network are determined. By applying proper scale factors the corresponding natural frequencies of the mechanical shaft system are readily computed.

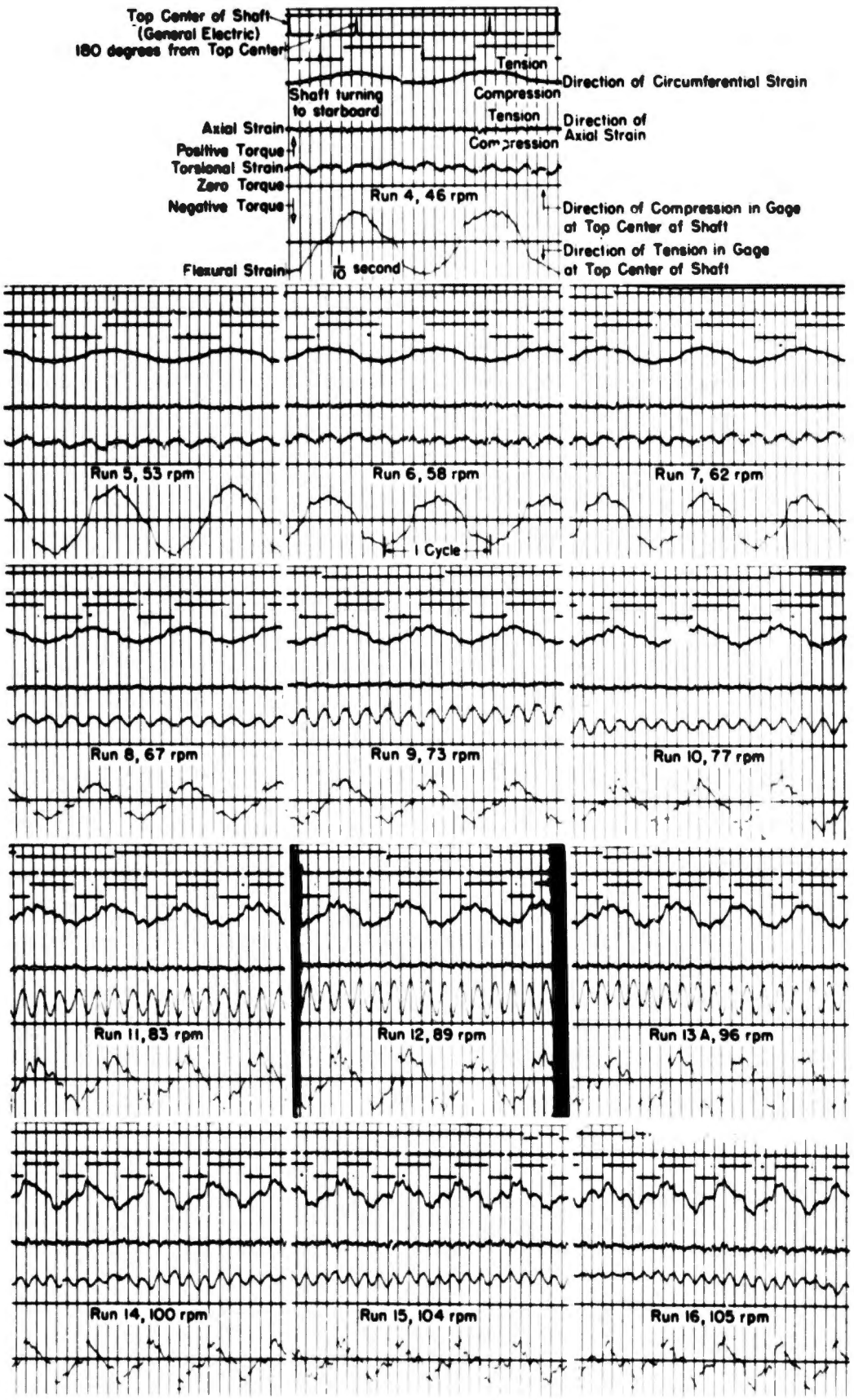


Figure 13a - Ship in Light Condition of Loading (Propeller Partially Submerged)

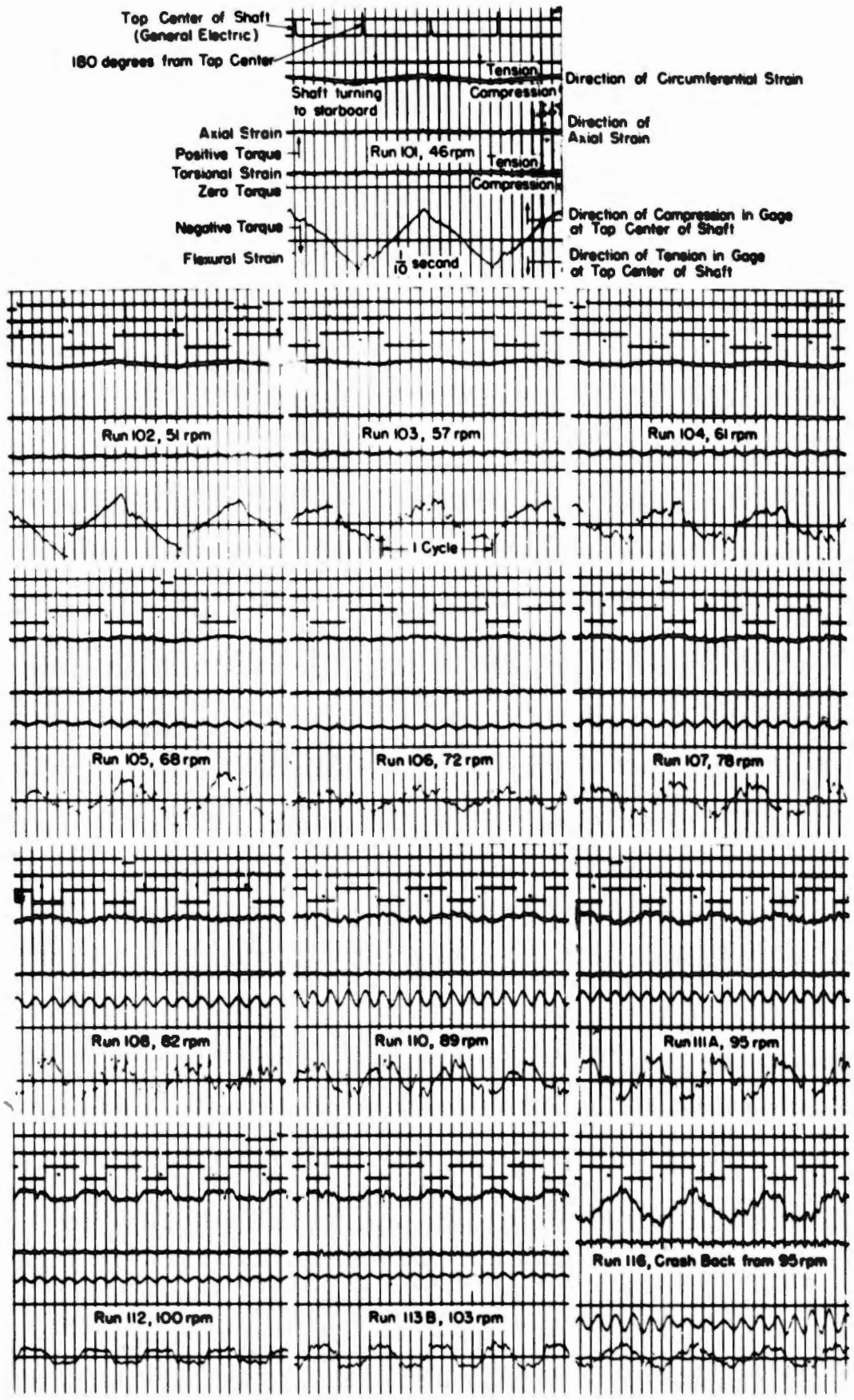


Figure 13b - Ship in Load Condition

Figure 13 - Sample Oscillograms Obtained During Sea Tests

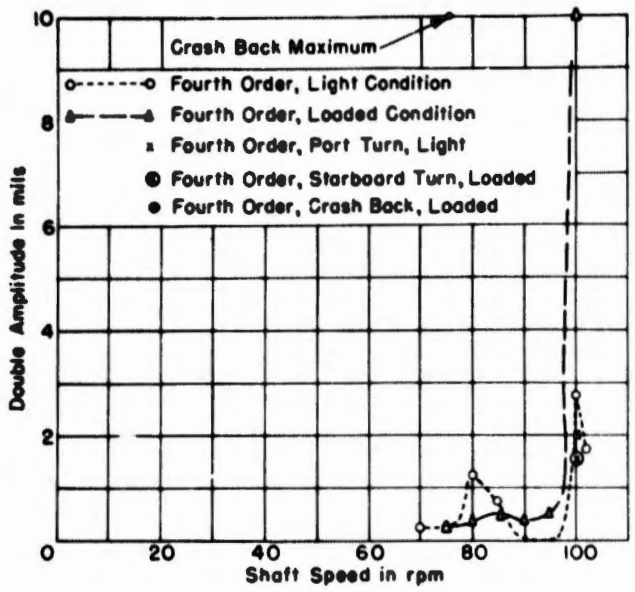


Figure 14a - Vertical Vibration

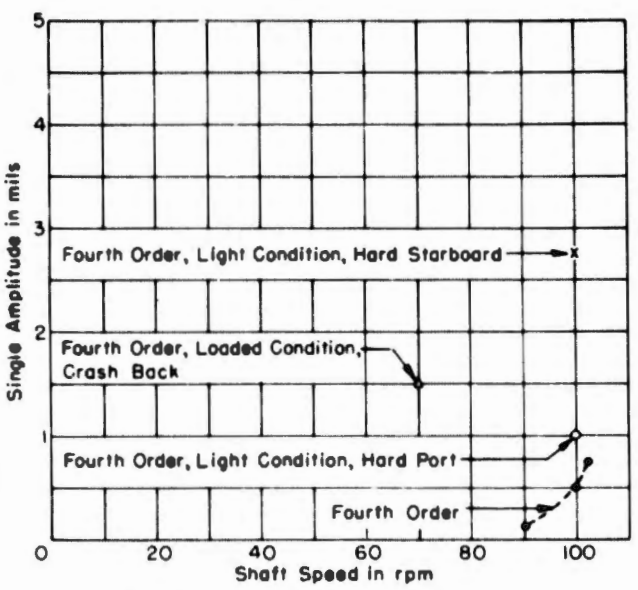


Figure 14b - Transverse Vibration

Figure 14 - Hull Vibration Measured on the Fantail

The prime factors affecting the natural frequencies are the effective locations and restraints of the bearings and bearing supports as well as the virtual mass of water acting with the propeller. It is probable that the bearing support locations change with the snip's speed and loading. The effect of such variations on the natural frequency has been studied by means of an electrical analog and the results are shown in Figure 15. The shaft was supported as shown in the sketch of Figure 15, and the bearings were assumed to be restrained so as to preclude linear deflection. The actual shaft arrangement for the T-2 tanker is shown in Figure 16. It is quite evident that the natural frequency decreases rapidly as the support is moved away from the propeller. Table 2 gives the natural frequencies determined by the analog for a number of assumed conditions.

The wide range of natural frequencies obtained for the several assumptions made emphasizes the futility of attempting to determine, with accuracy, the natural frequencies of lateral vibration unless the indeterminancies as to the supports can be resolved. The more general methods of analysis are very helpful, however, in a qualitative study of the effects that changes in selected parameters cause in the behavior of the system.

A simple formula for the fundamental natural whirling frequencies of propeller-shaft systems has been derived[11] from dynamic considerations; it has been reduced to a readily usable form which requires only the application of the methods of statics. This formula has been applied to propeller-shafts of

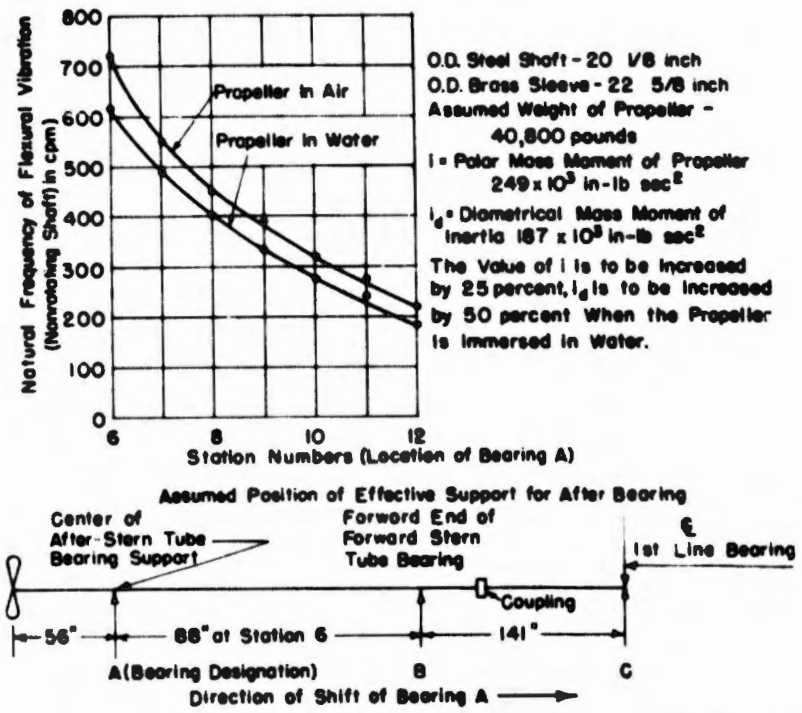


Figure 15 - Natural Frequency of Lateral Vibration As a Function of Location of Bearing Support

TABLE 2

Comparison of Frequency Values Determined for Several Assumed Conditions

| Case | Condition | Method | Forward Whirl | Counter Whirl | Nonrotating Shaft |
|---|---|---|---|---|---|
| 1 | 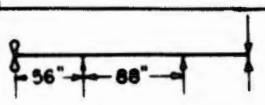  | Electrical Analog | *666 | *576 | *612 |
| 2 | 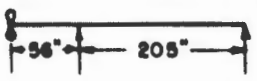  | do | *660 | *576 | *612 |
| 3 |   | do | *750 | *636 | *684<br>**810 |
| 4a | Vibration Generator Test (Horizontal) | Experiment on T-2 Tanker | - | - | **890<br>*680 |
| 4b | Vibration Generator Test (Vertical) | do | - | - | **1100<br>*820 |

*Propeller immersed in water.

**Propeller in air.

the T-2 tanker and the Liberty ship in order to permit a direct check against the experimentally determined values of the natural frequencies.

Assume that the propeller-shaft system is represented by Figure 17 in which the propeller has been replaced by a disk. The terminology and sign convention which is to be used with the "whirling" formula as well as the formula itself are also given in this figure. The assumptions made in the derivation of the expression for the natural frequency are that the shaft is spinning with uniform angular velocity, that the rigidity of the shafting system is the same in all planes containing the shaft axis and that the effect of the mass of the shaft and of gravity may be neglected. The effects of bearing flexibility may be included in the computation of the influence coefficients.

Examination of the whirling formula shows that there are two natural whirling frequencies for each value of $\frac{\omega}{\Omega} = h$, where $\omega$ is the angular velocity of shaft spin and $\Omega$ is the angular velocity of whirl. That is for each absolute value of h there may exist four natural frequencies of whirl. Two of these four modes of vibration represent a whirl in the direction of spin, and two correspond to a whirl opposite in direction to that of the spin, i.e., a counterwhirl. A more general treatment of flexural shaft vibration is given in Reference 11.

The formula given in Figure 17 has been used to calculate the natural frequencies of whirling and of flexural vibration of the propeller-shaft system of the T2-SE-A2 tanker and of the Liberty ships; the results are given in Table 3. The computations were made for several conditions of shaft support; the flexibility of the bearings was not taken into consideration. Case 4 of Table 3 does give a natural frequency of 1070 cpm for the nonspinning shaft (h = 0) in air. This figure practically coincides with the measured natural frequency of 1100 cpm in the vertical plane as determined by the vibration generator tests. The full-scale tests gave values of 820 and 680 cpm for the natural frequencies of the nonrotating propeller-shaft system immersed in water, for the horizontal and vertical directions respectively, thus indicating nonuniform bearing flexibility.

The eighth-order whirling resonances, as evidenced by harmonic analysis of the strain data, occurred near 840 cpm (forward whirl) and 720 cpm (counterwhirl). The theory of the whirling shaft[11] indicates that the natural frequency is lower for the counterwhirl than for the forward whirl; see also the data in Table 3.

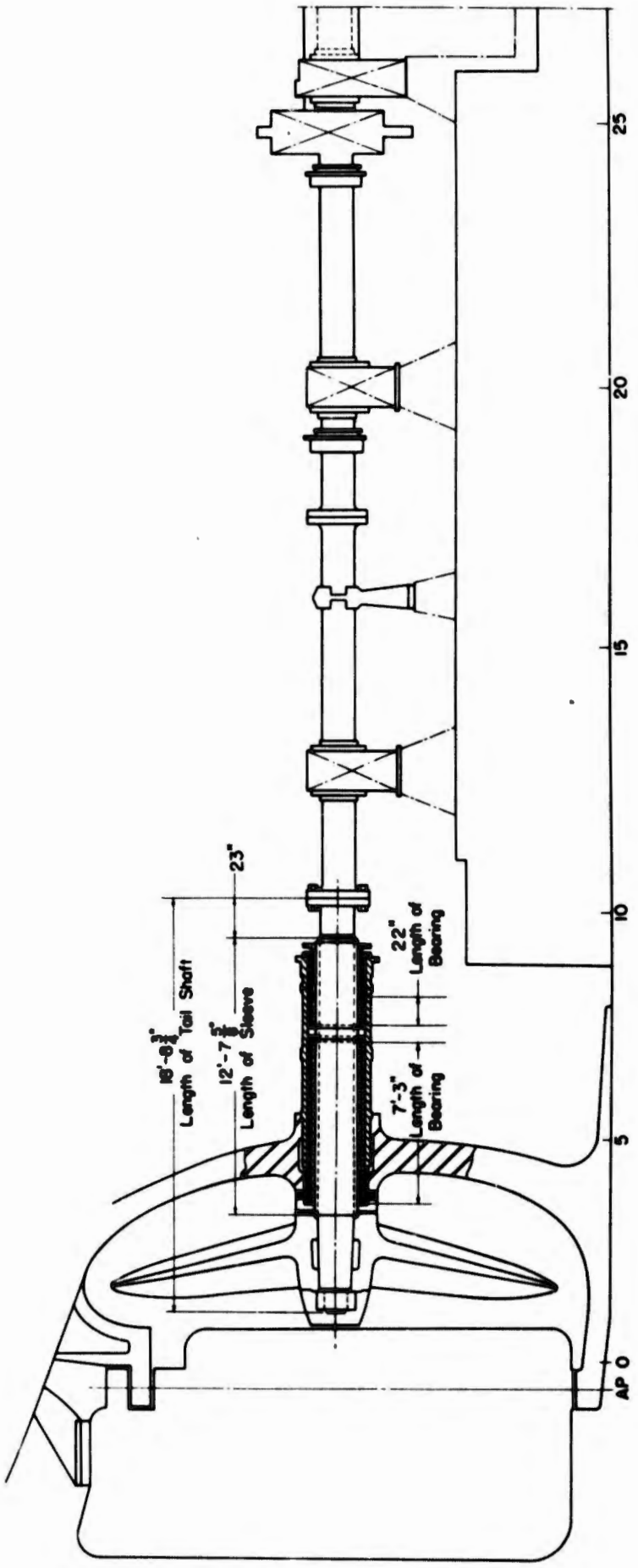


Figure 16 - Arrangement of Shafting

TABLE 3

**Natural Whirling Frequencies Computed for Several Assumed Shaft Systems for a T-2 Tanker and a Liberty Ship**

| Type of Ship | Assumed Shaft System | System in Air or Water | Natural Frequency** of Whirl (cpm) for the Indicated Value of h | | | | | | | |
|---|---|---|---|---|---|---|---|---|---|---|
| | | | +1 | +1/4 | +1/8 | 0 | -1/8 | -1/4 | -1 | ←h |
| T-2 (MISSION) Tanker† | 1 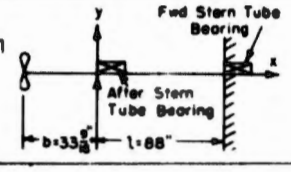  | Air | | | | 1450<br>7230 | | | | 1st Mode<br>2nd Mode |
| | | Water | 3056<br>i* | 1380<br>6920 | | 1220<br>6660 | | 1100<br>6520 | 888<br>6320 | 1st Mode<br>2nd Mode |
| | 2 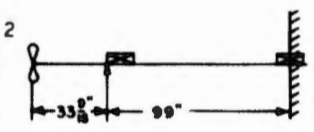  | Air | | | | 1399<br>7049 | | | | 1st Mode<br>2nd Mode |
| | | Water | | 1340<br>6750 | | 1190<br>6490 | | 1070<br>6350 | | 1st Mode<br>2nd Mode |
| | 3 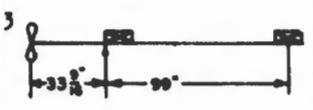  | Air | | | | 1290<br>6890 | | | | 1st Mode<br>2nd Mode |
| | | Water | | 1240<br>6592 | | 1098<br>6328 | | 996<br>6176 | | 1st Mode<br>2nd Mode |
| | 4 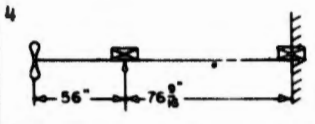  | Air | | | | 1070<br>4320 | | | | 1st Mode<br>2nd Mode |
| | | Water | 1540<br>1 | 1020<br>4130 | 975<br>3980 | 934<br>3857 | 894<br>3770 | 859<br>3697 | 717<br>3459 | 1st Mode<br>2nd Mode |
| Libertyt† | 5 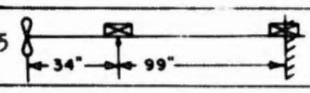  | Water | 1220<br>5410 | 1110<br>4910 | 1035<br>4650 | 974<br>4490 | 922<br>4360 | 876<br>4280 | 695<br>4010 | 1st Mode<br>2nd Mode |

*i denotes an imaginary root.

**The error due to the neglect of the mass of the shaft is of the order of 1 percent. The relationship used to calculate the natural whirling frequencies is the formula given in Figure 17.

†The physical constants used in the calculations for the T-2 Tanker were:

in air $m = 106$ lb-sec$^2$ in. $i = 249{,}000$ lb-sec$^2$ in. $i_d = 187{,}000$ lb-sec$^2$ in. $EI = 31.4 \times 10^{10}$ lb-in$^3$

in water $m = 116$ $i = 312{,}000$ lb-sec$^2$ in. $i_d = 280{,}000$ lb-sec$^2$ in.

where m is the mass of the propeller, i and $i_d$ its mass moment of inertia about a polar axis and a diametric axis respectively.

††The physical constants used in the calculations for the Liberty ship were:

in water $m = 63$ lb-sec$^2$ in., $i = 144{,}000$ lb-sec$^2$ in., $i_d = 100{,}000$ lb-sec$^2$ in., $EI = 9.9 \times 10^{10}$ lb-in$^3$

## 6.2. TORSIONAL STRESSES

The strain data showed the presence of a definite fourth-order (blade frequency) torsional strain variation superimposed on a static strain. The stresses calculated from the strains are plotted in Figure 18 on the basis of propeller shaft rpm. It is seen from an inspection of this figure that the values of the alternating and static torsion stresses are about equal to each other at 90 shaft rpm for the light condition. The shaft system has a resonant torsional frequency of vibration of about 360 cpm; the resonance therefore falls within the operating rpm of the vessel.

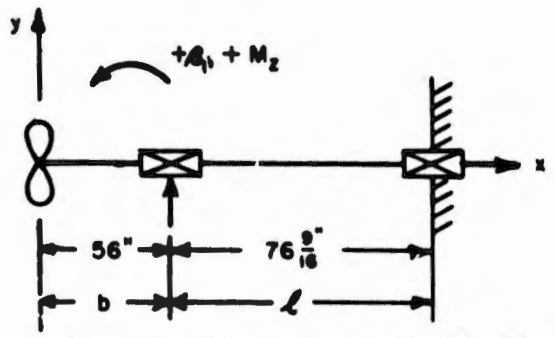


Figure 17 - Schematic Diagram of Shaft Disk System

The influence coefficients $\delta_P$, $\delta_M$, $\theta_P$, $\theta_M$ must be given the proper sign.

Let $\Omega_N$ be the natural angular whirling frequency,

$m$ be the mass of the disk (propeller),

$h = \frac{\omega}{\Omega}$ is the ratio of the spin velocity to the whirling velocity,

$i_d$ is the mass moment of inertia of the disk about a diameter,

$i_P$ is the polar mass moment of inertia of the disk,

$k = \frac{i_P}{i_d}$ is the ratio of polar to diametrical mass moment of inertia,

$G = i_d(kh-1)$ is an effective inertia (the gyroscopic term),

$y$ and $\beta_1$ are the linear and angular deflections of the disk, respectively,

$\delta_P$ is the static deflection at the disk due to a unit transverse force applied to the disk,

$\delta_M$ is the static deflection at the disk due to a unit moment applied to the disk about a transverse axis,

$\theta_P$ is the static rotation of the disk about a transverse axis due to a unit transverse load applied to the disk, and

$\theta_M$ is the static rotation of the disk about a transverse axis due to a unit moment applied to the disk about that transverse axis.

$$\Omega_N^2 = \frac{(m\delta_P - \theta_M G) \pm \sqrt{(m\delta_P - \theta_M G)^2 - 4mG(\delta_M\theta_P - \delta_P\theta_M)}}{2mG(\delta_M\delta_P - \delta_P\theta_M)} \quad \text{(Whirling Formula)}$$

This formula will, in general, give two whirling frequencies for each value of h. For a derivation of this formula and a general discussion of the whirling phenomenon, see Reference 11.

The steady and alternating components of the torsional stresses are tabulated in Tables 4 and 5 for the light and loaded conditions respectively. It is to be noted that, although the steady component of the stress is greatest for the load condition, the alternating stress components are about twice as high for the light as for the loaded condition. This increase of the vibratory torsional stress, observed for the lesser drafts, is undoubtedly due to the fact that almost half the propeller projected from the water, (see Figure 10), during operation in the light condition, resulting in large variations in torque.

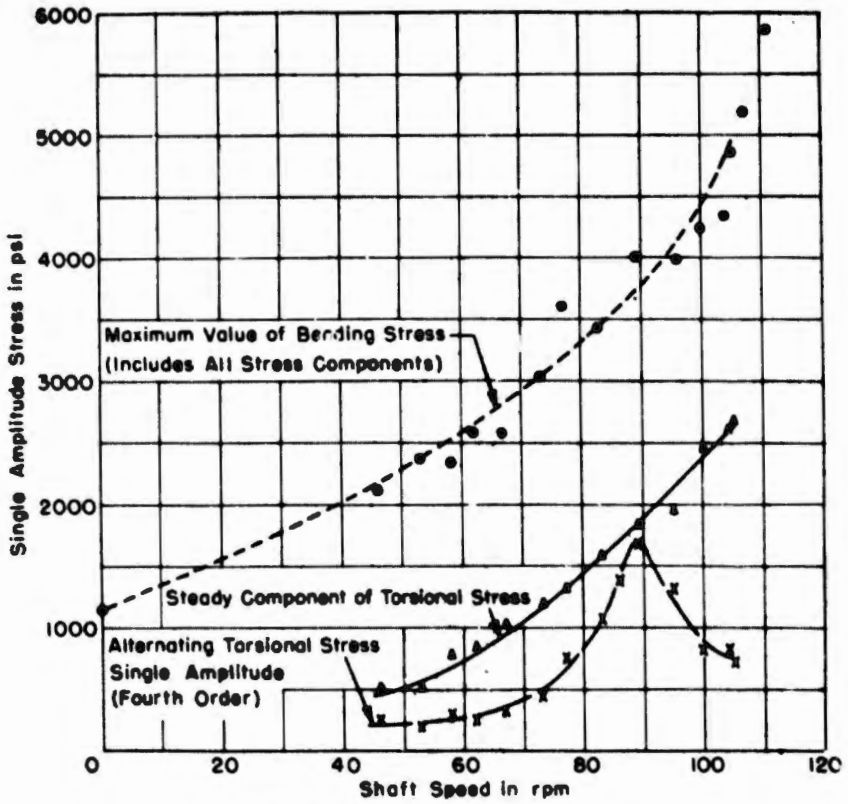


Figure 18a - Light Condition

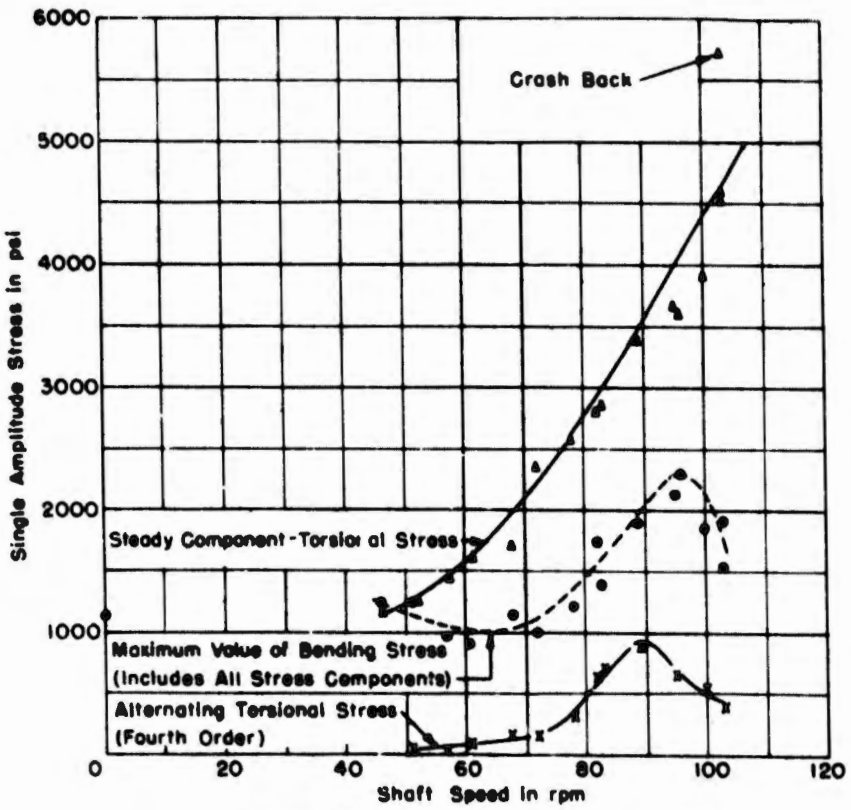


Figure 18b - Load Condition

Figure 18 - Torsion and Bending Stresses in the Propeller Shaft

The stress values pertain to the strain gage location.

TABLE 4

Stresses in Tailshaft for the Light Condition

| Run Number | Shaft rpm | Bending Stress (Maximum) psi | Angular Position at Which Maximum Bending Stress was Measured* degrees | Torsion Stress (Maximum) psi | Axial** | | Principal Combined Stresses*** | |
|---|---|---|---|---|---|---|---|---|
| | | | | | Thrust lb | Stress psi | Steady Component Only psi | Maximum Value psi |
| 4 | 46 | ±2110 | +10 | 510 ± 250 | $.270 \times 10^2$ | -80 | 580 | 2210 |
| 5 | 53 | ±2370 | +8 | 500 ± 210 | $379 \times 10^2$ | -110 | 550 | 2700 |
| 6 | 58 | ±2340 | +10 | 780 ∓ 280 | $450 \times 10^2$ | -130 | 850 | 2800 |
| 7 | 62 | ±2580 | -5 | 840 ∓ 270 | $520 \times 10^2$ | -150 | 920 | 2960 |
| 8 | 67 | ±2580 | +17 | 1040 ∓ 330 | $611 \times 10^2$ | -170 | 1130 | 3040 |
| 9 | 73 | ±3040 | +12 | 1190 ∓ 460 | $725 \times 10^2$ | -210 | 1300 | 3760 |
| 10 | 77 | ±3620 | +8 | 1330 ∓ 780 | $809 \times 10^2$ | -230 | 1450 | 4720 |
| 11 | 83 | ±3430 | +20 | 1580 ∓1070 | $952 \times 10^2$ | -270 | 1720 | 4920 |
| 12 | 89 | ±4010 | +15 | 1840 ∓1690 | $1103 \times 10^2$ | -320 | 2000 | 5900 |
| 13A | 96 | ±3980 | +15 | 1950 ∓1330 | $1270 \times 10^2$ | -370 | 2130 | 5200 |
| 13B | 96 | ±3530 | +18 | 1850 ∓1080 | $1300 \times 10^2$ | -370 | 2040 | 5380 |
| 14 | 100 | ±4250 | 0 | 2470 ∓ 830 | $1418 \times 10^2$ | -410 | 2680 | 5550 |
| 15 | 104 | ±4350 | +15 | 2630 ∓ 830 | $1540 \times 10^2$ | -440 | 2850 | 5585 |
| 16 | 105 | ±4880 | 0 | 2680 ∓ 720 | $1600 \times 10^2$ | -460 | 2910 | 6350 |
| 17 | Port Turn | ±4400 | - | 2380 ∓ 720 | | ≈ -400 | 2590 | 5730 |
| 18 | Starboard Turn | ±5060 | - | 2810 ∓ 560 | | ≈ -400 | 3020 | 6680 |
| 3B | 107 | ±5190 | - | 2520 ∓ 930 | $1626 \times 10^2$ | -510 | 2790 | 6320 |
| 3C | 111 | ±5860 | - | 2520 ∓ 930 | $1770 \times 10^2$ | -560 | 3120 | 7290 |

*Angular position refers to the position of a reference blade from the vertical (positive in direction of rotation).

**The thrust values are obtained from model test data. The axial stresses were computed from the thrust data.

***Formula used is

$$\text{Combined Maximum Principal Stress} = \frac{\sigma}{2} + \sqrt{\left(\frac{\sigma}{2}\right)^2 + \tau_s^2}$$

where $\sigma$ is the normal stress (axial and bending) and $\tau_s$ is the shear stress (torsion).

TABLE 5

Stresses in Tailshaft for the Load Condition

| Run Number | Shaft rpm | Bending Stress (Maximum) psi | Torsion Stress (Maximum) psi | Axial* | | Principal Combined Stresses** | |
|---|---|---|---|---|---|---|---|
| | | | | Thrust lb | Stress psi | Steady Component Only psi | Maximum Value psi |
| 101 | 46 | ±1240 | 1170 ± 0 | 342 ×10² | -105 | 1230 | 2080 |
| 102 | 51 | ±1240 | 1250 ± 80 | 413 ×10² | -130 | 1320 | 2190 |
| 103 | 57 | ± 970 | 1450 ± 80 | 510 ×10² | -160 | 1530 | 2060 |
| 104 | 61 | ± 890 | 1610 ± 115 | 580 ×10² | -180 | 1700 | 2310 |
| 105 | 68 | ±1140 | 1720 ± 155 | 719 ×10² | -225 | 1840 | 2750 |
| 106 | 72 | ± 990 | 2350 ± 165 | 802 ×10² | -255 | 2480 | 2740 |
| 107 | 78 | ±1210 | 2570 ± 330 | 953 ×10² | -300 | 2720 | 3690 |
| 108 | 82 | ±1740 | 2790 ± 660 | 1072 ×10² | -335 | 2970 | 4300 |
| 109 | 83 | ±1380 | 2840 ± 710 | 1110 ×10² | -350 | 3020 | 4020 |
| 110 | 89 | ±1890 | 3390 ± 880 | 1331 ×10² | -420 | 3610 | 4080 |
| 111A | 95 | ±2120 | 3670 ± 660 | 1630 ×10² | -520 | 3940 | 5360 |
| 111B | 96 | ±2300 | 3590 ± 630 | 1698 ×10² | -535 | 3870 | 5720 |
| 112 | 100 | ±1840 | 3920 ± 550 | 1945 ×10² | -610 | 4230 | 5550 |
| 113A | 103 | ±1530 | 4530 ± 390 | 2150 ×10² | -675 | 4890 | 6020 |
| 113B | 103 | ±1910 | 4610 ± 390 | 2150 ×10² | -675 | 4960 | 6360 |
| 114 | Port Turn 100 | ±2490 | 4530 ± 390 | 1945 ×10² | -610 | 4850 | 6540 |
| 115 | Starboard Turn 95 | ±2770 | 3750 ±1720 | 1634 ×10² | -515 | 3960 | 6690 |
| 116 | Crash Back 85 | ±5720 | 5700 ±3100 | | ≈-200 | 5700 | 10,470 |

*The thrust values are obtained from model test data. The axial stresses were computed from the thrust data.

**Formula used is

$$\text{Combined Maximum Principal Stress} = \frac{\sigma}{2} + \sqrt{\left(\frac{\sigma}{2}\right)^2 + \tau_s^2}$$

where $\sigma$ is the normal stress (axial and bending) and $\tau_s$ is the shear stress (torsion).

The torsional vibration measurements made with the Geiger torsiograph did not indicate a torsional resonance; this may be ascribed to the low magnitude of the measured vibratory signal. This emphasizes the fact that large vibratory stresses are not necessarily associated with easily observable vibratory motions. It may therefore be difficult to discover the presence of large vibratory stresses by means of vibration measurements alone. The largest torsional stress was measured during the crash-back operation, load condition, and had a value of $5700 \pm 3100$ psi. The largest value obtained during the steady-speed runs was measured at 89 rpm, light condition, and had a value of $1840 \pm 1690$ psi.

## 6.3. BENDING STRESSES

Analysis of the strain data shows that the bending stresses in the tailshaft are fairly complex in character but that the first-order component is by far the most predominant. Sample oscillograms are shown in Figure 13. For each test condition a typical oscillogram was analyzed into its Fourier components, up to and including the eleventh-order term. The Fourier analysis was carried out by a 48-ordinate scheme for the light-displacement condition and by means of the "Reeves Electronic Analog Computer" (REAC) for the heavy-displacement condition. The results of this harmonic analysis are presented in Table 6.

The magnitude of the phase angle $\psi$ given in Table 6 may be utilized to show that:

A. For the light displacement the center of pressure is below the center of the propeller; thus the first-order bending stresses due to the overhanging weight of the propeller (less the buoyant force) and those due to the eccentrically applied thrust are additive.

B. For the heavy displacement the location of the center of pressure varies appreciably with shaft rpm. It lies, however, in the first quadrant of the propeller. In this case the gravity effects tend to neutralize the bending stresses due to the eccentrically applied thrust.

The position of the center of thrust and the magnitude of the applied bending moment due to the eccentrically applied thrust may be calculated in any particular case by the method indicated in Figure 19. In this figure, the magnitudes of the static components of $M_g$ and $M_{gp}$ as well as the orientation of these vectors are obtained from the test data, Table 6. The result of a series of such calculations is indicated in Figure 20.

**Run 13-A**

Light Condition - 96 rpm
Thrust = 127,000 lb

$M_{g_p}$ = 800 x 3430 = 2750 x $10^3$ in-lb

$M_g$ = 800 x 1150 = 920 x $10^3$ in-lb

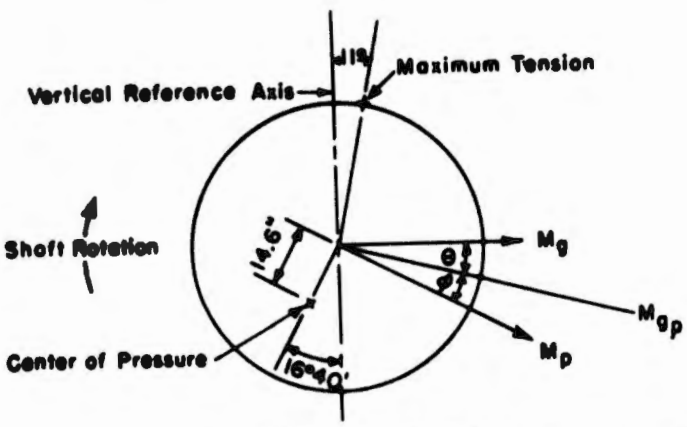


$M_g$ = Bending moment due to gravity and buoyancy loads (Vector)

$M_p$ = Bending moment due to eccentrically applied thrust P (Vector)

$M_{g_p} = M_g + M_p$ (Vectors)

Section modulus of shaft = 800 $in^3$

$M_p \sin\phi = M_g \sin\theta$

$M_p \cos\phi = M_{g_p} - M_g \cos\theta$

$$\therefore \tan\phi = \frac{M_g \sin\theta}{M_{g_p} - M_g \cos\theta} = \frac{176}{1850} = 0.095$$

$\phi$ = 5° - 40'

$$\therefore M_p = \frac{176 \times 10^3}{0.0987} = 1{,}860{,}000 \text{ in-lb}$$

$$\text{Location of Center of pressure} = d = \frac{1.86 \times 10^6}{0.127 \times 10^6} = 14.6"$$

**Run 111-A**

Load Condition - 95 rpm
Thrust = 163,000 lb

$M_{g_p}$ = 800 x 1255 = 1,004,000 in-lb

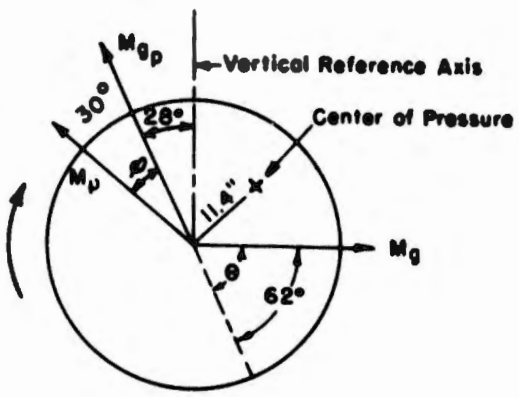


$M_p \sin\phi = M_g \sin\theta$

$M_p \cos\phi - M_g \cos\theta = M_{g_p}$

$$\therefore \tan\phi = \frac{M_g \sin\theta}{M_{g_p} + M_g \cos\theta} = 0.238$$

$\phi$ = 29° - 28'

$$\therefore M_p = \frac{81.1 \times 10^4}{0.492} = 1{,}650{,}000 \text{ in-lb}$$

$$\text{Location of Center of pressure} = d = \frac{1.65 \times 10^6}{0.163 \times 10^6} = 10.1"$$

Figure 19 - Calculation of the Center of Pressure and Magnitude of Bending Moment Due to Eccentrically Applied Static Component of Thrust

The externally applied static bending moment, $M_g$, due to the weight of the propeller less the buoyant force, results in a bending stress at the strain-gage location which has a frequency of one cycle per shaft revolution. The measured value of this bending stress is 1150 psi and the corresponding bending moment is 920,000 in-lb. Since the weight of the propeller less the buoyant force is about 37,300 lb, the effective point of application of this

# TABLE 6

## Harmonic Analysis of Strain Oscillograms

**The oscillogram records analyzed are shown in Figure 13.**

| Run Number | RPM | Peak Stress psi | Harmonics* | | | | | | | | | | | | | | | | | | | |
|---|---|---|---|---|---|---|---|---|---|---|---|---|---|---|---|---|---|---|---|---|---|---|
| | | | Steady Term | | 1st Harmonic | | 2nd Harmonic | | 3rd Harmonic | | 4th Harmonic | | 5th Harmonic | | 6th Harmonic | | 7th Harmonic | | 8th Harmonic | | 9th Harmor | |
| | | | $A_0$ psi | Percent Peak Stress | $A_1$ psi | Percent Peak Stress | $A_2$ psi | Percent Peak Stress | $A_3$ psi | Percent Peak Stress | $A_4$ psi | Percent Peak Stress | $A_5$ psi | Percent Peak Stress | $A_6$ psi | Percent Peak Stress | $A_7$ psi | Percent Peak Stress | $A_8$ psi | Percent Peak Stress | $A_9$ psi | Perce Peak Stres |
| 3-C | 111 | 5610 | 240 | 4.3 | 3760 | 67 | 135 | 2.4 | 1400 | 24 | - | - | 800 | 14 | 200 | 4 | 210 | 4 | - | - | 530 | 9 |
| 4 | 46 | 2030 | 57 | 2.8 | 2015 | 99 | 60 | 3.0 | 190 | 9 | 90 | - | 130 | 6 | 40 | - | 55 | 2 | 15 | - | 40 | 2 |
| 5 | 53 | 2370 | 32 | 1 | 2330 | 98 | 155 | 7 | 225 | 9 | 90 | - | 130 | 6 | 105 | - | 70 | 3 | 60 | - | 60 | 2 |
| 6 | 58 | 2310 | 130 | 6 | 2210 | 96 | 50 | 2 | 210 | 9 | 50 | - | 150 | 9 | 10 | - | 105 | 4 | 25 | - | 80 | 3 |
| 7-1 | 62 | 2265 | 100 | 4 | 2040 | 90 | 15 | - | 275 | 12 | 75 | - | 75 | 3 | 50 | 2 | 50 | 2 | 45 | - | 25 | 1 |
| 7-2 | 62 | 2580 | 130 | 5 | 2450 | 95 | 90 | 3 | 300 | 12 | 40 | - | 225 | 9 | 50 | - | 55 | 2 | 35 | - | 50 | - |
| 8 | 67 | 2580 | 230 | 9 | 2420 | 94 | 70 | 3 | 235 | 9 | 10 | - | 210 | 8 | 15 | - | 195 | 7 | 40 | - | 135 | 5 |
| 9 | 73 | 3040 | 190 | 6 | 2635 | 87 | 45 | 2 | 235 | 8 | 30 | 2 | 375 | 12 | 25 | 1 | 150 | 5 | 20 | - | 15 | 4 |
| 10-1 | 77 | 3620 | 238 | 7 | 3000 | 83 | 60 | 2 | 570 | 16 | 20 | - | 125 | 32 | 55 | 1 | 175 | 5 | 20 | - | 180 | 8 |
| 11 | 83 | 3360 | 267 | 8 | 2700 | 80 | 35 | 1 | 330 | 10 | 70 | - | 400 | 12 | 65 | - | 270 | 9 | 55 | - | 250 | 9 |
| 12 | 89 | 3860 | 360 | 9 | 3140 | 79 | 165 | 4 | 570 | 38 | 100 | 3 | 310 | 8 | 55 | - | 275 | 8 | 25 | - | 395 | 13 |
| 13-A | 96 | 3980 | 266 | 7 | 3430 | 86 | 260 | 6 | 525 | 13 | 90 | - | 530 | 14 | 45 | - | 260 | 7 | 60 | - | 125 | 4 |
| 14 | 100 | 4000 | 578 | 14 | 3150 | 79 | 57 | 1 | 900 | 21 | 86 | - | 388 | 10 | 62 | - | 220 | 6 | 32 | - | 232 | 8 |
| 15 | 104 | 3760 | 355 | 9 | 2450 | 65 | 140 | 4 | 1210 | 32 | 52 | - | 295 | 8 | 62 | - | 155 | 5 | 87 | - | 345 | 12 |
| 16-1 | 105 | 3750 | 290 | 8 | 1870 | 50 | 154 | 4 | 1300 | 35 | 170 | 5 | 310 | 9 | 125 | 3 | 703 | 22 | 182 | 6 | 155 | 5 |
| 17 | 104 | 3630 | - | - | 2120 | 58 | 50 | 1 | 675 | 19 | - | - | 850 | 25 | - | - | 245 | 8 | - | - | 310 | 11 |
| 101 | 46 | 1200 | - | - | 925 | 77 | 25 | 2 | 85 | 7 | - | - | 55 | 5 | - | - | 45 | 4 | - | - | 20 | 2 |
| 102 | 51 | 1240 | - | - | 845 | 68 | 20 | 2 | 135 | 11 | - | - | 100 | 8 | - | - | 75 | 6 | - | - | 40 | 3 |
| 103 | 57 | 965 | - | - | 760 | 78 | 45 | 5 | 110 | 11 | - | - | 95 | 10 | - | - | 55 | 6 | - | - | 25 | 3 |
| 104-1 | 67 | 755 | - | - | 590 | 78 | 25 | 3 | 115 | 15 | - | - | 110 | 10 | - | - | 65 | 7 | - | - | 35 | 5 |
| 104-2 | 61 | 505 | - | - | 135 | 27 | 45 | 9 | 150 | 30 | - | - | 70 | 14 | - | - | 120 | 24 | - | - | 70 | 14 |
| 105 | 68 | 1105 | - | - | 860 | 78 | 45 | 4 | 165 | 15 | - | - | 65 | 6 | - | - | 25 | 2 | - | - | 35 | 3 |
| 106 | 72 | 905 | - | - | 645 | 71 | 65 | 7 | 170 | 19 | - | - | 170 | 19 | - | - | 70 | 8 | - | - | 45 | 6 |
| 107 | 73 | 1210 | - | - | 910 | 75 | 95 | 8 | 115 | 9 | - | - | 20 | 2 | - | - | 145 | 36 | - | - | 195 | 16 |
| 108 | 82 | 1535 | - | - | 1230 | 80 | 80 | 5 | 90 | 6 | - | - | 195 | 13 | - | - | 110 | 7 | - | - | 215 | 14 |
| 110 | 89 | 1785 | - | - | 1150 | 64 | 60 | 3 | 490 | 27 | - | - | 140 | 8 | - | - | 255 | 14 | - | - | 240 | 13 |
| 111-A | 95 | 1910 | 90 | 5 | 1255 | 66 | 90 | 5 | 155 | 8 | 30 | - | 240 | 13 | 80 | - | 230 | 12 | 35 | 2 | 300 | 16 |
| 111-A Sample 2 | 95 | 1850 | | | 1010 | 55 | | | 840 | 45 | | | 305 | 16 | | | 160 | 9 | | | | |
| 112 | 100 | 1630 | - | - | 1600 | 98 | 35 | 2 | 520 | 32 | - | - | 210 | 13 | - | - | 240 | 15 | - | - | 170 | 10 |
| 113-B | 103 | 1640 | - | - | 1550 | 95 | 70 | 4 | 290 | 18 | - | - | 110 | 7 | - | - | 140 | 10 | - | - | 135 | 11 |
| 115 | 92 | 2765 | - | - | 1260 | 46 | 80 | 3 | 925 | 34 | - | - | 450 | 16 | - | - | 95 | 3 | 125 | 5 | 60 | 3 |
| 116 | 85 | 5630 | - | - | 4400 | 78 | 185 | 3 | 680 | 12 | 260 | 3 | 515 | 9 | 160 | 3 | 315 | 6 | 215 | 3 | 250 | 4 |

*Subscript n of $A_n$ denotes the order of the harmonic. The second figure gives the stress as a percentage of the peak stress.

**Stress = $A_0 + \sum A_n \sin(n\ t + \psi n)$. The phase angles for Runs 3-C - 17 are referred to the top dead center position; those for Run.

Oscillograms

own in Figure 13.

| | Harmonics* | | | | | | | | | | | | | | | | | | | |
|---|---|---|---|---|---|---|---|---|---|---|---|---|---|---|---|---|---|---|---|---|
| nic ent ss | 4th Harmonic | | 5th Harmonic | | 6th Harmonic | | 7th Harmonic | | 8th Harmonic | | 9th Harmonic | | 10th Harmonic | | 11th Harmonic | | 1st Harmonic $\psi_1$ | 2nd Harmonic $\psi_2$ | 3rd Harmonic $\psi_3$ | 4th Harmonic $\psi_4$ |
| | $A_4$ psi | Percent Peak Stress | $A_5$ psi | Percent Peak Stress | $A_6$ psi | Percent Peak Stress | $A_7$ psi | Percent Peak Stress | $A_8$ psi | Percent Peak Stress | $A_9$ psi | Percent Peak Stress | $A_{10}$ psi | Percent Peak Stress | $A_{11}$ psi | Percent Peak Stress | | | | |
| | - | - | 800 | 14 | 200 | 4 | 210 | 4 | - | - | 530 | 9 | - | - | 250 | 4 | 77.4 | 345.6 | 69.2 | 100.9 |
| | 90 | - | 130 | 6 | 40 | - | 55 | 2 | 15 | - | 40 | 2 | 10 | - | 65 | 3 | 81.6 | 276.5 | 271.2 | 60.2 |
| | 90 | - | 130 | 6 | 105 | - | 70 | 3 | 60 | - | 60 | 2 | 50 | - | 70 | 3 | 79.0 | 187.0 | 155.7 | 355.0 |
| | 50 | - | 150 | 9 | 10 | - | 105 | 4 | 25 | - | 80 | 3 | 10 | - | 35 | 1 | 78.6 | 291.0 | 264.5 | 63.3 |
| | 75 | - | 75 | 3 | 50 | 2 | 50 | 2 | 45 | - | 25 | 1 | 15 | - | 25 | 1 | 86.2 | 305.6 | 125.7 | 128.7 |
| | 40 | - | 225 | 9 | 50 | - | 55 | 2 | 35 | - | 50 | - | 10 | - | 30 | - | 81.6 | 323.2 | 181.5 | 183.1 |
| | 10 | - | 210 | 8 | 15 | - | 195 | 7 | 40 | - | 135 | 5 | 55 | - | 35 | - | 75.3 | 200.8 | 204.3 | 339.4 |
| | 30 | 2 | 375 | 12 | 25 | 1 | 150 | 5 | 20 | - | 15 | 4 | 60 | 2 | 55 | 2 | 83.9 | 224.2 | 205.0 | 59.6 |
| | 20 | - | 125 | 32 | 55 | 1 | 175 | 5 | 20 | - | 180 | 8 | 45 | - | 135 | 5 | 87.6 | 207.8 | 119.4 | 275.4 |
| | 70 | - | 400 | 12 | 65 | - | 270 | 9 | 55 | - | 250 | 9 | 20 | - | 50 | 2 | 75.0 | 238.6 | 128.4 | 338.0 |
| | 100 | 3 | 310 | 8 | 55 | - | 275 | 8 | 25 | - | 395 | 13 | 150 | 5 | 50 | 1 | 77.2 | 179.3 | 115.2 | 251.0 |
| | 90 | - | 530 | 14 | 45 | - | 260 | 7 | 60 | - | 125 | 4 | 135 | 4 | 75 | 3 | 79.2 | 222.8 | 185.9 | 38.2 |
| | 86 | - | 388 | 10 | 62 | - | 220 | 6 | 32 | - | 232 | 8 | 53 | - | 362 | 13 | 75.2 | 258.8 | 97.9 | 158.9 |
| | 52 | - | 295 | 8 | 62 | - | 155 | 5 | 87 | - | 345 | 12 | 100 | 4 | 120 | 5 | 77.5 | 321.3 | 92.7 | 70.4 |
| | 170 | 5 | 310 | 9 | 125 | 3 | 703 | 22 | 182 | 6 | 155 | 5 | - | - | 235 | 9 | 97.7 | 124.0 | 79.7 | 214.0 |
| | - | - | 850 | 25 | - | - | 245 | 8 | - | - | 310 | 11 | - | - | 60 | 2 | 85.1 | 184.5 | 129.6 | 17.0 |
| | - | - | 55 | 5 | - | - | 45 | 4 | - | - | 20 | 2 | - | - | 15 | 1 | 89.0 | 9.9 | 128.4 | 317.0 |
| | - | - | 100 | 8 | - | - | 75 | 6 | - | - | 40 | 3 | - | - | 40 | 3 | 104.5 | 202.4 | 124.5 | - |
| | - | - | 95 | 10 | - | - | 55 | 6 | - | - | 25 | 3 | - | - | 20 | 2 | 121.0 | 242.9 | 67.4 | - |
| | - | - | 110 | 10 | - | - | 65 | 7 | - | - | 35 | 5 | - | - | 35 | 5 | 117.8 | 46.7 | 23.4 | - |
| | - | - | 70 | 14 | - | - | 120 | 24 | - | - | 70 | 14 | - | - | 70 | 14 | 105.2 | 34.4 | 258.4 | - |
| | - | - | 65 | 6 | - | - | 25 | 2 | - | - | 35 | 3 | - | - | 30 | 3 | 86.6 | 252.3 | 163.7 | - |
| | - | - | 170 | 19 | - | - | 70 | 8 | - | - | 45 | 6 | - | - | 85 | 9 | 70.1 | 175.7 | 141.9 | - |
| | - | - | 20 | 2 | - | - | 145 | 36 | - | - | 195 | 16 | - | - | 60 | 5 | 69.2 | 223.3 | 326.6 | - |
| | - | - | 195 | 13 | - | - | 110 | 7 | - | - | 215 | 14 | - | - | 90 | 6 | 115.6 | 326.5 | 95.7 | - |
| | - | - | 140 | 8 | - | - | 255 | 14 | - | - | 240 | 13 | - | - | 90 | 5 | 84.0 | 308.8 | 195.1 | - |
| | 30 | - | 240 | 13 | 80 | - | 230 | 12 | 35 | 2 | 300 | 16 | 60 | 4 | 35 | 2 | 208.1 | 104.1 | 58.4 | 135.7 |
| | | | 305 | 16 | | | 160 | 9 | | | | | | | | | | | | |
| | - | - | 210 | 13 | - | - | 240 | 15 | - | - | 170 | 10 | - | - | 20 | 1 | 157.3 | 53.1 | 136.2 | - |
| | - | - | 110 | 7 | - | - | 140 | 10 | - | - | 135 | 11 | - | - | 20 | 1 | 150.7 | 122.3 | 76.9 | - |
| | - | - | 450 | 16 | - | - | 95 | 3 | 125 | 5 | 60 | 3 | 80 | - | 10 | - | 112.8 | 215.4 | 74.0 | - |
| | 260 | 3 | 515 | 9 | 160 | 3 | 315 | 6 | 215 | 3 | 250 | 4 | 215 | 3 | 165 | 3 | 126.2 | 205.1 | 104.4 | 66.6 |

second figure gives the stress as a percentage of the peak stress.

Runs 3-C - 17 are referred to the top dead center position; those for Runs 101 - 116 are referred to arbitrary reference positions.

| | Phase Angle in Degrees** | | | | | | | | | | |
|---|---|---|---|---|---|---|---|---|---|---|---|
| onic $\phi_1$ | 2nd Harmonic $\phi_2$ | 3rd Harmonic $\phi_3$ | 4th Harmonic $\phi_4$ | 5th Harmonic $\phi_5$ | 6th Harmonic $\phi_6$ | 7th Harmonic $\phi_7$ | 8th Harmonic $\phi_8$ | 9th Harmonic $\phi_9$ | 10th Harmonic $\phi_{10}$ | 11th Harmonic $\phi_{11}$ | Notes |
| .4 | 345.6 | 69.2 | 100.9 | 137.2 | 10.9 | 64.0 | 158.7 | 350.0 | 73.1 | 302.6 | Light Condition (see Table 1) |
| .6 | 276.5 | 271.2 | 60.2 | 51.6 | 253.4 | 126.8 | 33.5 | 54.6 | 184.9 | 83.5 | do |
| .0 | 187.0 | 155.7 | 355.0 | 9.0 | 149.9 | 109.6 | 293.3 | 219.0 | 82.8 | 56.9 | do |
| .6 | 291.0 | 264.5 | 63.3 | 45.0 | 209.1 | 118.1 | 344.7 | 308.7 | 196.8 | 34.2 | do |
| .2 | 305.6 | 125.7 | 128.7 | 127.7 | 191.7 | 29.2 | 255.3 | 125.6 | 248.1 | 82.5 | do |
| .6 | 323.2 | 181.5 | 183.1 | 27.1 | 1.6 | 140.2 | 100.7 | 318.2 | 265.2 | 321.3 | do |
| .3 | 200.8 | 204.3 | 339.4 | 14.1 | 147.3 | 65.2 | 312.2 | 217.9 | 192.9 | 28.1 | do |
| .9 | 224.2 | 205.0 | 59.6 | 56.5 | 309.1 | 83.5 | 270.0 | 312.5 | 152.4 | 340.8 | do |
| .6 | 207.8 | 119.4 | 275.4 | 158.8 | 198.2 | 1.6 | 150.7 | 74.8 | 181.3 | 246.0 | do |
| .0 | 238.6 | 128.4 | 338.0 | 349.7 | 323.5 | 358.1 | 209.0 | 89.7 | 260.0 | 214.1 | do |
| .2 | 179.3 | 115.2 | 251.0 | 282.9 | 78.0 | 1.6 | 237.4 | 12.5 | 178.7 | 356.0 | do |
| .2 | 222.8 | 185.9 | 38.2 | 9.0 | 205.4 | 55.3 | 49.8 | 37.3 | 296.6 | 334.8 | do |
| .2 | 258.8 | 97.9 | 158.9 | 197.0 | 57.2 | 88.3 | 358.3 | 12.0 | 155.1 | 55.3 | do |
| .5 | 321.3 | 92.7 | 70.4 | 114.9 | 73.2 | 16.4 | 214.9 | 340.5 | 315.7 | 332.4 | do |
| .7 | 124.0 | 79.7 | 214.0 | 158.0 | 324.0 | 129.[illegible] | 86.0 | 91.0 | 69.0 | 102.3 | do |
| .1 | 184.5 | 129.6 | 17.0 | 59.2 | 92.0 | 178.4 | 27.0 | 209.6 | 315.0 | 86.1 | do |
| .0 | 9.9 | 128.4 | 317.0 | 309.8 | 315.0 | 120.5 | 45.0 | 92.6 | 344.0 | 77.9 | Loaded Condition (see Table 1) |
| .5 | 202.4 | 124.5 | - | 93.9 | - | 71.1 | - | 65.3 | - | 39.8 | do |
| .0 | 242.9 | 67.4 | - | 54.7 | - | 89.0 | - | 14.6 | - | 235.5 | do |
| .8 | 46.7 | 23.4 | - | 354.2 | - | 325.6 | - | 144.1 | - | 146.3 | do |
| .2 | 34.4 | 258.4 | - | 218.1 | - | 275.8 | - | 36.6 | - | 333.4 | do |
| .6 | 252.3 | 163.7 | - | 59.6 | - | 202.6 | - | 65.5 | - | 120.0 | do |
| .1 | 175.7 | 141.9 | - | 72.1 | - | 162.8 | - | 6.6 | - | 257.6 | do |
| .2 | 223.3 | 326.6 | - | 59.9 | - | 48.0 | - | 127.3 | - | 86.1 | do |
| .6 | 326.5 | 95.7 | - | 24.3 | - | 216.8 | - | 61.1 | - | 135.0 | do |
| .6 | 308.8 | 195.1 | - | 106.5 | - | 60.1 | - | 45.3 | - | 39.7 | do |
| .1 | 104.1 | 58.4 | 135.7 | 25.2 | 103.5 | 346.5 | 22.0 | 277.5 | 298.3 | 237.7 | do |
| | | | | | | | | | | | do |
| .5 | 53.1 | 136.2 | - | 132.1 | - | 73.9 | - | 50.7 | - | 188.1 | Loaded Condition (see Table 1) |
| .7 | 122.3 | 76.9 | - | 117.3 | - | 101.6 | - | 131.6 | - | 158.2 | do |
| .8 | 215.4 | 74.0 | - | 121.6 | - | 33.5 | - | 109.0 | - | 152.0 | Turn - Loaded Condition |
| .2 | 205.1 | 104.4 | 66.6 | 186.9 | 167.8 | 62.5 | 87.1 | 114.2 | 187.4 | 16.0 | Crash Back - Loaded Condition |

rary reference positions.

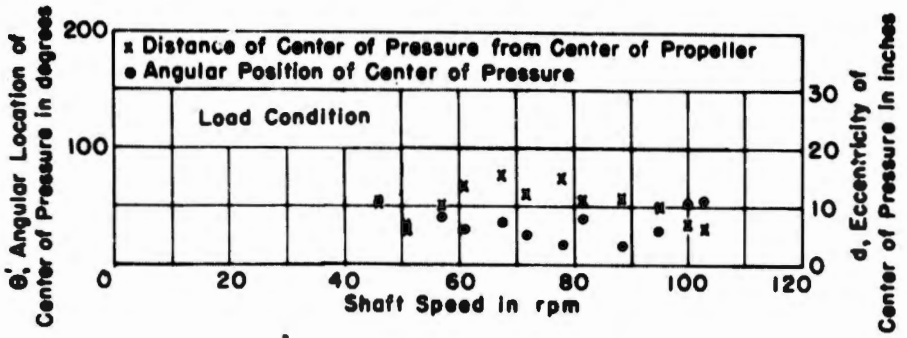


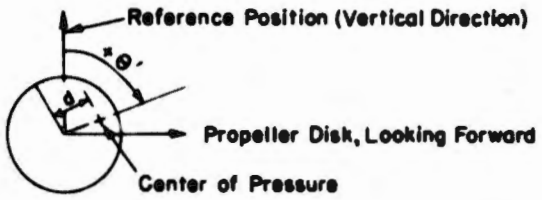


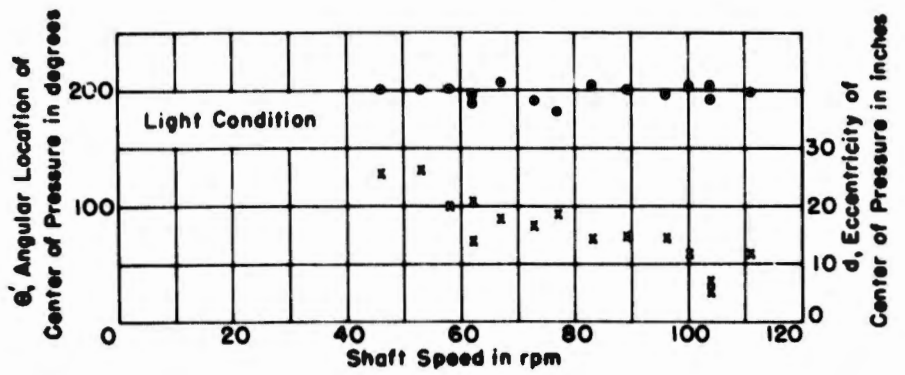


Figure 20 - Location of the Center of Pressure, Computed by the Method Illustrated in Figure 19

weight is computed on the basis of measured strain to be about 24.6 inches aft of the gage location. The center of the propeller is approximately 22.9 inches aft of the gage location. Comparison of these figures provides a check on the accuracy of the strain measurements.

The alternating bending stresses measured with the SR-4 strain gages are plotted in Figures 18a and 18b on a basis of shaft rpm for the light and load conditions, respectively. It is evident from an inspection of these figures that, for the light condition, the bending stress is the predominant one and, for the same rpm, is always larger than the bending stress for the load condition. Conversely, for the load condition the combined torsion stress predominates and, for the same rpm, is always larger than the corresponding torsion stress for the light condition.

It has been stated before in this section that, for the light condition, the first-order bending stresses due to the eccentric thrust and those due to the weight of the propeller reinforce one another; the variations of bending stress with rpm would therefore be expected to have the general form actually obtained, providing that there were no serious resonant flexural shaft vibrations. It might therefore be concluded that no serious flexural resonances are present, without resorting to further examination of the Fourier components of the bending stress. However, the alternating bending stress for the load condition does not vary in an obviously logical pattern; a possible explanation may be found through an examination of the harmonic content of the bending stresses together with a study of the location of the center of pressure.

The results of a harmonic analysis of the bending stresses, given in Table 6, are also plotted in graphical form in Figure 21. This analysis shows, as does an inspection of the actual oscillograms, that the harmonic components of the stresses do vary somewhat even though the propeller speed is kept reasonably constant. Wherever curves are drawn in Figure 21, they are intended to show the probable maximum value that would be measured if the oscillograms had been taken over a long period of time. For the light condition definite eighth-order whirling resonances are indicated at about 90 rpm (counterwhirl, 720 cpm) and at 105 rpm (forward whirl, 840 cpm). For the load condition the higher-order stress variations were of rather small magnitude; only one fairly well-defined resonance was apparent, namely an eighth-order counterwhirl (ninth-order strain) at about 90 rpm.

The shape of the bending stress curve for the load condition in Figure 18b may be explained by noting that the minimum stress value at 60 rpm coincides with a minimum value of the first-order stress near 60 rpm; see Figure 21a. The reason for the low first-order stress near 60 rpm is that the vector sum of the bending moment due to gravity loads and the first-order bending moment due to the eccentrically applied thrust is a minimum. This behavior could conceivably be utilized in design by locating the center of thrust so as to make the bending moment due to the applied thrust counteract that caused by the propeller weight at the operating propeller rpm. The hump in the stress curve near 95 rpm in Figure 18b is due to the relatively large contributions of the third- and ninth-order harmonics near this speed.

The higher-order odd harmonics of the bending stress correspond to whirling motions of the shaft as discussed in Section 2 and Reference 11. A theoretical analysis of the bending moment acting on a propeller has been made and some of the results will be given here.

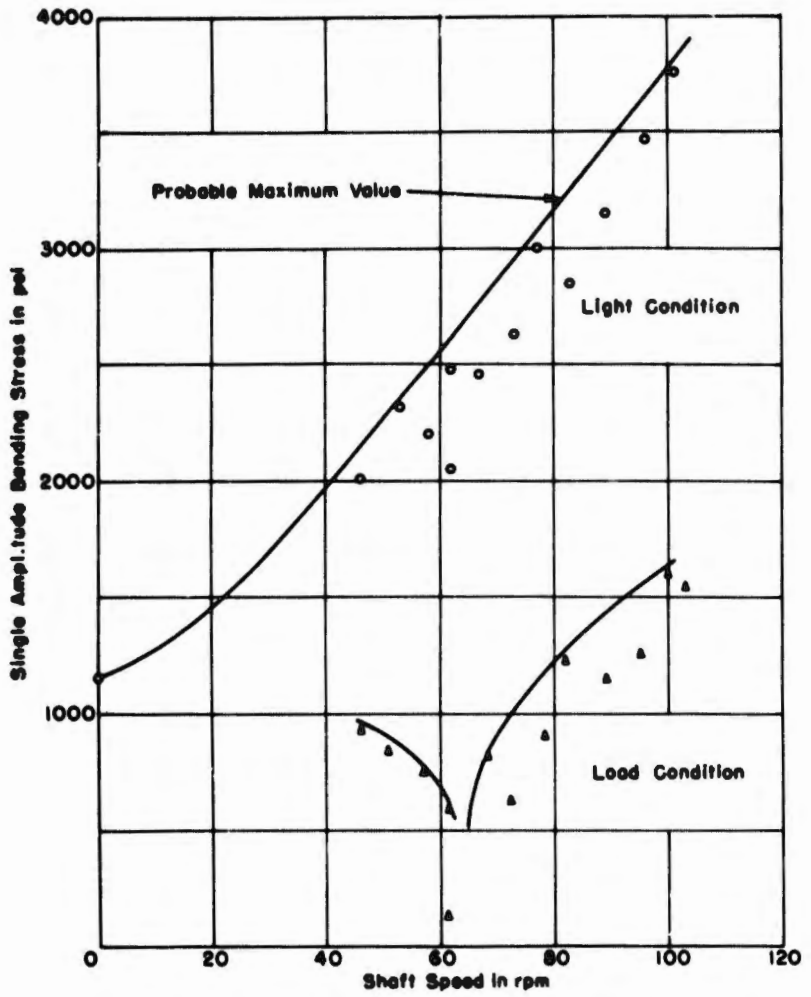


Figure 21a - First-Order Component of Bending Stresses

The curves drawn are not mean values of points plotted, but are intended to show probable maximum values that would be measured if measurements had been taken over a sufficiently long period of time.

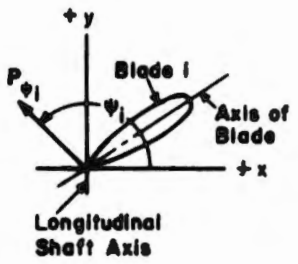


Let $P_{\psi_i}$ denote the moment vector representing the bending moment acting at the root of blade i in a plane containing the axes of the blade and of the shaft. This vector will rotate with the blade with an angular velocity $\omega$. $\psi_i = \omega t$ is the angular spatial position of $P_{\psi_i}$, and t is the time elapsed from some reference time.

The bending moment acting on each blade may be expressed as a Fourier series in $\omega t$. The contributions of the several blades may then be added to give the resulting moment acting on the propeller disk. Carrying out this analysis, it is found that the frequencies of the bending moment variations acting on the propeller disk are equal to $kn\omega$ where k is any integer, n is the number of blades, and $\omega$ is the angular spin velocity of the propeller.

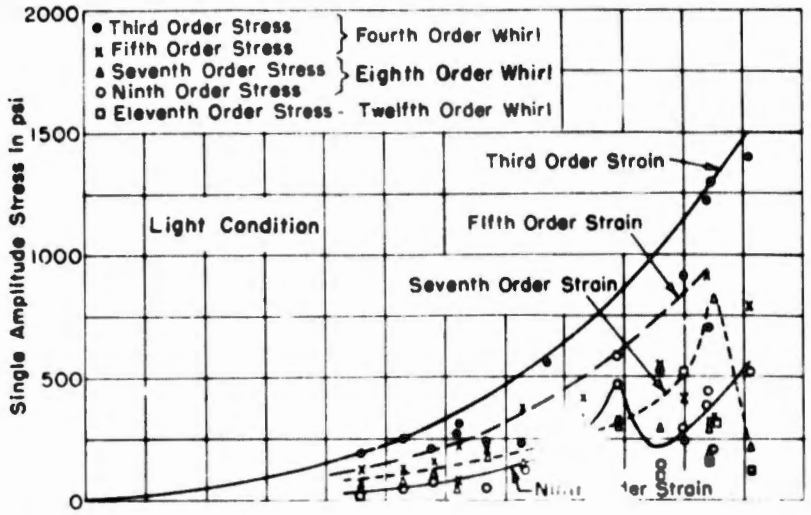


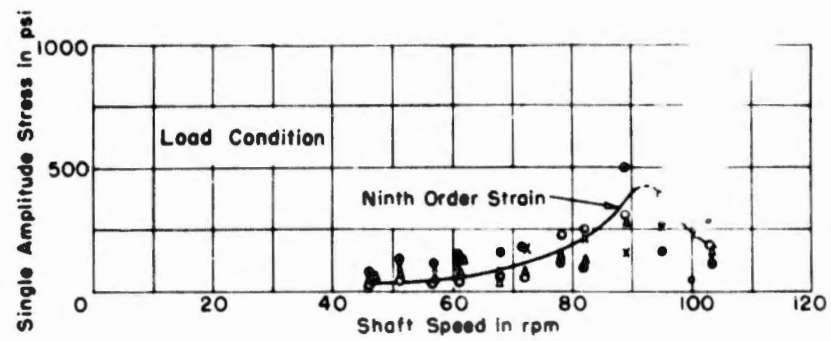


Figure 21b - Higher-Order Components of Bending Stresses

The seventh- and ninth-order strain variations correspond to eighth-order forward and counterwhirls respectively.

Figure 21 - Bending Stresses - Harmonic Components

For a propeller with an even number of blades only the coefficients of the odd harmonics in the Fourier series for $P_{\phi_i}$ will give rise to higher-order moments, whereas for a propeller with an odd number of blades only the coefficients of the even harmonics of this Fourier series need be considered in determining the whirling motions. For the four-bladed propellers installed on the T-2 tankers only even orders of moment variation and whirls, and consequently odd orders of strain, would be expected. The harmonic analysis of the strain records showed this to be essentially true. These results will be given on page 40 for a four-bladed propeller.

| | | | | | |
|---|---|---|---|---|---|
| Fourier Component of $P_\phi$ | 1 | 3<br>5 | 7<br>9 | 11<br>13 | All even orders |
| Fourier Component of Total Bending Moment Acting on the Propeller (Referred to a set of axes fixed in the ship) | 0 | 4 | 8 | 12 | None |
| Order of Strain Variation Referred to Shaft rpm (Whirl in direction of shaft rotation) | 1* | 3 | 7 | 11 | None |
| (Whirl in direction opposite to shaft rotation) | 1* | 5 | 9 | 13 | None |

*No whirl.

The vibration-generator tests showed that the nonrotating propeller-shaft system has natural frequencies of flexural vibration in the horizontal and vertical directions of 680 and 820 cpm respectively, for the submerged conditions. It is indicated in Sections 2 and 6.1 that the rotation of the propeller may induce two whirling resonances corresponding to each flexural resonance of the nonro ating shaft system. The higher-order flexural resonances indicated in Figure 21b correspond to such whirling resonances although it will not be possible to check the resonance frequencies by analytical methods because knowledge is lacking as to the magnitude of a number of physical quantities that significantly do affect these frequencies.

To recapitulate some of the major items discussed in this section: It has been shown that the first-order bending stress variation predominates and that the eccentr c application of thrust increases the alternating bending stresses for the light condition and tends to decrease these stresses for the load condition. The higher-order bending stresses associated with shaft whirling are generally of greater magnitude for the light than for the load condition but their contribution relative to the first-order bending stress is greater for the load condition. The ship's operating speed of 90 rpm coincides, for the load condition, with a condition of relatively high third- and ninth-order bending stresses although the magnitude of the alternating bending stress is not severe for the load condition. The highest bending stresses were observed during the "crash back" operation, i.e., going astern from full-power ahead; the value of the measured bending stress was approximately $\pm 5700$ psi.

## 6.4. COMBINED STRESSES

The maximum value of the combined stress is tabulated, for each of the test conditions, in Tables 4 and 5. These values were obtained as follows. Each oscillogram was examined in order to find that particular instant at which the resultant of the shearing and normal stresses gave a maximum value of the combined stress. A plot of the combined stresses against shaft rpm is shown in Figure 22.

Examination of Figure 22 shows a rather definite peak of stress near 90 rpm for the light condition. This peak is due to the effect of the first-mode torsional resonance at 90 rpm as is evident from Figure 18a. The occurrence of the torsional resonance within the normal operating range is, of course, undesirable. For the load condition the combined stresses increase with the rpm and do not indicate the presence of severe resonance effects.

The combined stresses computed from the strain components measured during the hard turns were of the order of 10 percent higher than during a straight run at the same shaft rpm. The stresses obtained during the crash-back operation were severe, with a maximum value of about 10,500 psi for the loaded condition. The crash-back operation was not carried out for the light condition, but it would be logical to expect even more severe stresses for this condition. One might estimate, on the basis of the measurements, that the combined stresses during crash-back are about twice the maximum stresses obtained during normal, constant-speed operation.

It is of interest to determine the principal directions of the maximum normal tensile stresses inasmuch as a fatigue failure would probably occur in the plane on which this stress acts. The principal direction, calculated for the most severe stress condition for both light and loaded operations, was at an angle of 21 degrees with the shaft axis for Run 3C and at an angle of 31 degrees for Run 116.

It should be remembered that the strains were measured at a location which was relatively free of stress concentration. The actual peak stresses in the tailshaft probably occur near the end of the keyway since it is here that stress concentration due to the effect of discontinuities and end effects (fretting,* corrosion, shrink fit) of the propeller hub and liner will be greatest. The shaft failures are due to the combined effects of torsion, bending, and axial stresses, all of which do have both steady and alternating components The bending stress predominates on the T-2 tankers. It is difficult to determine the endurance strength under such combined loads, primarily because little

*The word fretting as used in this report describes a mechanical vibratory rubbing motion between two contacting surfaces.

is known about the behavior of materials under these conditions. So-called "stress concentration factors" due to surface discontinuities can be determined analytically, but their influence, under conditions of alternating loads, on the endurance strength is known to be less than theory would indicate. The stress concentration factors to be used in evaluating endurance strength are usually obtained from endurance tests conducted on special test specimens which are subjected to one type of load variation only. If steady and alternating loads are superimposed on each other, it is not clear whether or not a stress concentration factor should be applied to the steady as well as to the alternating-load component, although one would reason that it should be applied to both, provided the elastic limit is not exceeded.

If it were desired to determine the combined stress at a point, then assuming that all stresses are within the elastic limit, the expression for the shear and normal stresses acting on any given plane through the point could be written by expressing each stress component as a function of time and applying the proper stress concentration factor to every component whether steady or alternating. This procedure gives the magnitude and direction of the stresses but does not provide much useful information for determining the endurance strength of a structure. Probable maximum shear and principal stresses for some of the test runs were determined by applying a stress concentration factor of 2 to the steady and alternating torsion stresses.

In order to check the endurance strength of the shaft, an approach suggested by Soderberg,[14] which is based on experimental data, was used. Let it be assumed that the maximum shear theory of failure is valid, then failure will occur when the maximum shear stress is equal to the yield point in shear, which is one-half the yield point in tension $\sigma_y$ or

$$\frac{1}{2}\left[(\sigma_1 - \sigma_2)^2 + 4\tau^2\right]^{1/2} = \frac{1}{2}\sigma_y$$

(for bi-axial stress $\sigma_1$, $\sigma_2$ combined with shear stress $\tau$). For the case under consideration the circumferential stress is zero, and the expression becomes

$$\frac{1}{2}\left(\sigma^2 + 4\tau^2\right)^{1/2} = \frac{1}{2}\sigma_y \qquad [1]$$

where $\sigma$ is the normal stress and $\tau$ the shear stress on a given plane. Actually Equation [1] provides a failure criterion. If a known set of stresses $\sigma$ and $\tau$ is substituted in Expression [1], the value of the expression may be considered as an indication of the degree to which the failure stress $\frac{1}{2}\sigma_y$ has been approached. Soderberg[14] found that test data may be interpreted to show

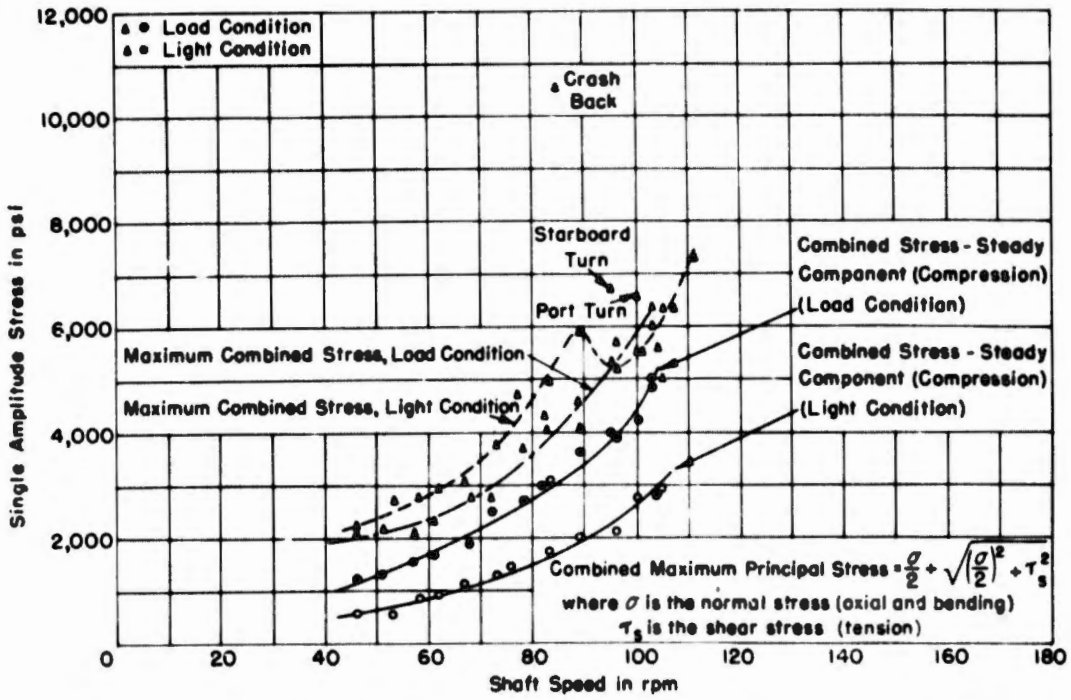


Figure 22 - Combined Stresses in the T-2 Tanker Shaft Computed from the Measured Strains

The stress values pertain to the strain gage location (see Figure 5).

that, for simultaneous application of a steady and an alternating stress, a fatigue failure would be likely to occur for the combinations

$$\frac{\tau_0}{\tau_y} + \frac{\tau_a}{\tau_e} \geq 1 \qquad [2]$$

where $\tau_0$ is the maximum steady value of resultant stress,

$\tau_a$ is the maximum alternating value of resultant stress,

$\tau_y$ is the yield point (static strength), and

$\tau_e$ is the endurance limit (endurance strength).

Note that in Expression [2] either shear stresses and (static) strength in shear or normal stresses and strength under normal stress are to be used, but not combinations of the two. In this discussion shear stresses and shear strength will be used. Expression [2] appears to be on the safe side and probably is nearly valid for the condition where both the alternating and steady components of stress act on the same plane. The steady and alternating components of the maximum shear stress are computed thus:

$$\tau_0^m = \frac{1}{2}\left[(K_t\,\sigma_0)^2 + 4(K_T\,\tau_0)^2\right]^{1/2}$$
$$\tau_a^m = \frac{1}{2}\left[(K_t\,\sigma_a)^2 + 4(K_T\,\tau_a)^2\right]^{1/2} \qquad [3]$$

where $K_t$ and $K_T$ are the stress concentration factors for longitudinal and torsional stresses; the subscripts o, a denote steady and alternating components respectively. The values of $\tau_0^m$ and $\tau_a^m$ are substituted in [2] giving

$$\frac{\tau_0^m}{\tau_y} + \frac{\tau_a^m}{\tau_e} \leq 1$$

Expression [2] taken with the equality sign may be plotted as in Figure 23, thus showing that the result is a straight line. Points lying above this line may result in fatigue failures. It is believed that stress concentration factors should be applied to both the steady and the alternating stresses as indicated by [3]. The BuShips Design Data Sheet for Shafting[15] does not apply a stress concentration factor to the steady-stress component; the stress conditions computed on the basis of the formulas given in Reference 15 are given in Columns 3 and 4 of Table 7 for comparison with the values in Columns 5 and 6 of the same table, which were computed by use of Equations [3].

The stress concentration factors for bending and torsion are taken as 1 and 2 respectively in accordance with Reference 15. The values of the resultant steady and alternating components $\tau_0^m$, $\tau_a^m$ are listed in Table 7 and in addition are plotted in Figure 23. The endurance limit in shear is taken as 14,000 psi, and the elastic limit in shear is taken as $\frac{1}{2}(30{,}000) = 15{,}000$ psi.

Examination of Figure 23 shows that the stress conditions plotted are all within the endurance limit condition, the crash-back operation (Run 116) excepted. Since a backing operation, such as Run 116, occurs but rarely in the life of a vessel, it need not be considered from the standpoint of endurance strength although it is necessary to assure that the ultimate strength not be exceeded at any point on the shaft under all operating conditions. The question then arises as to the reason for the shaft failures. The only stress concentration factor used in these calculations was that one which was applied to take account of the keyway effect. No allowance was made for the effects of salt-water corrosion, press fits, temperature, fretting corrosion, or of internal stresses set up in the shafting material during manufacture or assembly. The direct macroscopic effects of shock loading, resonance conditions, and eccentric thrust are reflected in the measured strains and, therefore,

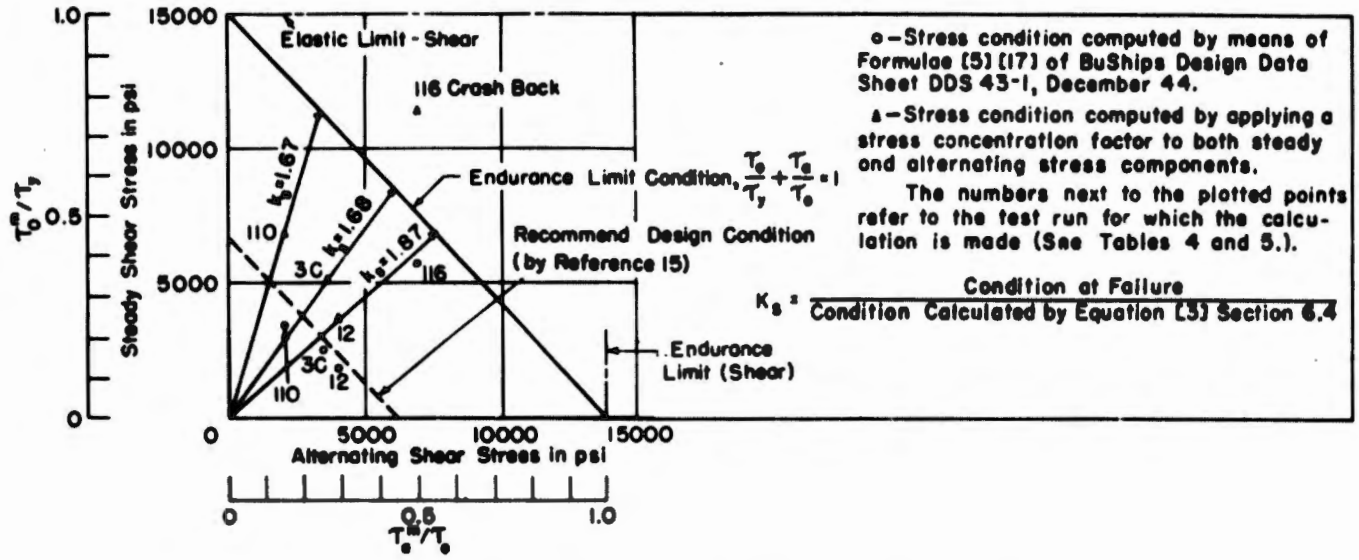


Figure 23 - Endurance Strength Diagram

TABLE 7

Stress Values used in Endurance Strength Calculation

| 1 | 2 | 3 | 4 | 5 | 6 | 7 | 8 | 9 | 10 |
|---|---|---|---|---|---|---|---|---|---|
| Run Number | Test Condition | *Stress Concentration Factor (K=2) Applied to Alternating Component Only | | Stress Concentration Factor ($K_T$ = 2) Applied to Both Steady and Alternating Components of Shear Stress, psi | | | | | |
| | | Steady Component psi | Alternating Component psi | Steady Component $\tau_0^m$ | Alternating Component $\tau_a^m$ | Maximum Shear Stress | Minimum Shear Stress | Maximum Principal Stress | Minimum Principal Stress |
| 3-C | 110 rpm Light | 5100 | ±6900 | 5100 | ±3450 | 7600 | 4200 | +10200 | -10600 |
| 12 | 89 rpm Light | 3700 | ±8000 | 3700 | ±4000 | 7400 | 1900 | +9300 | -9500 |
| 110 | 89 rpm Load | 6800 | ±4000 | 6800 | ±2000 | 8600 | 5100 | +9300 | -9700 |
| 116 | Crash Back Load | 11400 | ±13700 | 11400 | ±6900 | 17800 | 5900 | +20600 | -20800 |
| | | From Eq. [5] Ref. 15 | From Eq. [17] Ref. 15 | From Eq. [3] Sec. 6.4 | From Eq. [3] Sec. 6.4 | | | | |

*These values are equivalent tensile and compressive stresses which may be converted to shear stresses by multiplying the given values by the factor 1/2.

need not be considered by applying additional safety factors. The original tailshaft installed on the SAN LUIS OBISPO did show the presence of cracks under magnaflux examination. The special tailshaft used for the tests was magnafluxed after the test runs. This shaft did not evidence any cracks although it had been subjected to severe operating conditions, thus indicating that the shaft failures are due to a lack of endurance strength and not due to occasional overstressing.

It can be concluded from the foregoing discussion that the combined effects of fretting and salt-water corrosion and of residual and other stresses set up during assembly are sufficient to lower the endurance strength to an appreciable extent. It will be in order to raise the stress concentration factors applied to the stresses $\sigma$ and $\tau$ of Equations [3] in the preceding calculations to bring them into line with the failure condition, since it is known that failure does, in fact, occur. Then, in future design, such an augmented stress factor may be applied to the nominal stress in addition to known stress concentration factors in order to allow for these indeterminate but significant effects. Of course, if the contribution of each effect is known, they may all be combined to give the resultant factors $K_l$ and $K_T$ of Equations [3]. It would, of course, be preferable to eliminate fretting and similar deleterious actions altogether.

The factors by which the combined stress conditions, as calculated by Equations [3] using $K_l = 1$ and $K_T = 2$, must be multiplied in order to bring them up to the endurance failure condition are 1.67, 1.68, and 1.87 for runs 110, 3-C, and 12, respectively (see Figure 23). In order to furnish some margin of safety the design value for the combined stress condition should be less than that at the endurance limit. The required design condition may be expressed by the following formula

$$\frac{N\tau_0^m}{\tau_y} + \frac{N\tau_a^m}{\tau_e} = 1 \qquad [4]$$

where N is the safety factor, say 2, and $\tau_0^m$, $\tau_a^m$ are obtained from Equations [3].

On the basis of the foregoing, the following conclusions may be drawn. The ship's speed of 90 rpm coincides with a torsional resonance of the propeller-shafting system. The alternating stresses are more severe during the light condition, and the steady components are more severe during the load condition. The conditions for a fatigue failure are given approximately by Equation [2]. In using this relationship for shaft design it has been modified as in Equation [4]. The stress concentration factor for normal stresses

may be taken as 1.9 and that for torsion stresses as 2 × 1.9 = 3.8, for shafts similar to that of the T-2 tanker on the basis of the discussion just preceding and illustrated in Figure 23. Sometimes more accurate values of the stress factors may be determined. It is believed that the stress concentration factor should be applied to both the steady and the alternating components of the loads. The stresses due to resonant whirling of the shaft are not, as such, believed to be dangerous. The tailshaft failures of the T-2 tankers, and probably of similar classes as well, are due to a lack of endurance strength, not necessarily of the material but of the shaft as designed, built, and used. Some remedies for existing ships would be:

A. Reduce stress concentration and similar deleterious effects by preventing fretting between the propeller hub and the shaft at the forward end of the hub, by preventing fretting between the brass sleeve and the propeller shaft near the tapered end of the shaft, by excluding moisture from the highly stressed portions of the shaft, by care in the design and cutting of the keyway as well as by careful fitting of the propeller and key to the propeller shaft.

B. Increase the size of the tailshaft (a rather poor approach) in order to reduce the nominal stresses and/or select shaft materials, surface treatments, heat treatments, or shaft designs which will provide higher endurance strength for the intended service. Cold rolling and nitriding of press-fitted surfaces may be mentioned here.

C. Try to keep as much of the propeller immersed as possible.

Additional suggestions for new ship design would include:

A. Greater care should be taken in assuring relatively uniform flow over the entire propeller disk with special attention devoted to the position of the center of pressure relative to the center of the propeller. The prime objective is to reduce vibratory strains to a minimum.

B. The tailshaft design should take into consideration the endurance strength along the lines indicated in this section.

C. Computations should be made to assure that there will be no vibration resonances at the vessel's operating speeds.

Apart from the immediate problem there appears to be a definite need for information and utilization of information on (a) the relationship between endurance strength and various types of stress combinations, (b) the mechanics of initial crack formation, and (c) the effect of temperature on endurance strength in the presence of discontinuities. These questions are not directly

concerned with stress concentration factors due to geometric discontinuities such as may be studied by photoelastic methods. Valuable information could be derived from carefully planned experiments.

## 6.5. COMPARISON OF WAKE EFFECTS OBSERVED ON MODEL AND ON FULL-SCALE PROPELLERS

It has been mentioned before that the nonuniformity of the wake gives rise to periodic bending moments and torques which, in turn, cause periodic stress variations in the shaft.

In this section an attempt will be made to correlate the stresses and forces, which were calculated on the basis of model wake tests, with the values obtained from full-scale measurements. If a reasonable correlation can be shown to exist, then it may be practical to predict the stresses that will occur under operating conditions on the basis of model wake tests.

A model of the T-2 tanker was tested to determine the wake pattern under conditions approximating those existing during the full-scale trials for the load condition at 95 rpm. The wake data are given in Figure 24. The forces acting on the propeller blade due to this wake variation were computed for various angular positions of the blade. These forces were finally used to compute the resultant torque and bending moments at the strain gage location on the tailshaft, just forward of the propeller. These torque and moment variations, applied to the shaft, are plotted as Curves 6, 9, and 10 in Figure 25.

The moment due to the stress acting in the shaft would equal the applied moments if there were no dynamic effects present, that is, if these moments were applied statically. Owing to the presence of the dynamic effects it is necessary to multiply the applied moments by the applicable resonance factors in order to obtain the resisting moments in the shaft. The value of the resonance factor depends primarily on the damping, the ratio of the forcing frequency to the natural frequency, and the mode of vibration.

The strain oscillogram taken at 95 rpm, during the load condition, is reproduced in Figure 26. It is readily seen that the bending strain in the shaft does vary somewhat from cycle to cycle. Inspection of Sample 2, in conjunction with the analysis carried out so far shows it to be relatively free of higher-order resonance effects compared with the other cycles, and it was therefore chosen for comparison with the moment variation computed on the basis of the model wake tests (Curve 10 of Figure 25). Visual inspection of Sample 2, Figure 26, and Curve 10 of Figure 25 does show a good degree of similarity; it is to be expected, of course, that the strain records will contain

higher-order strains due to resonance effects which will be absent from the computed variations of Figure 25.

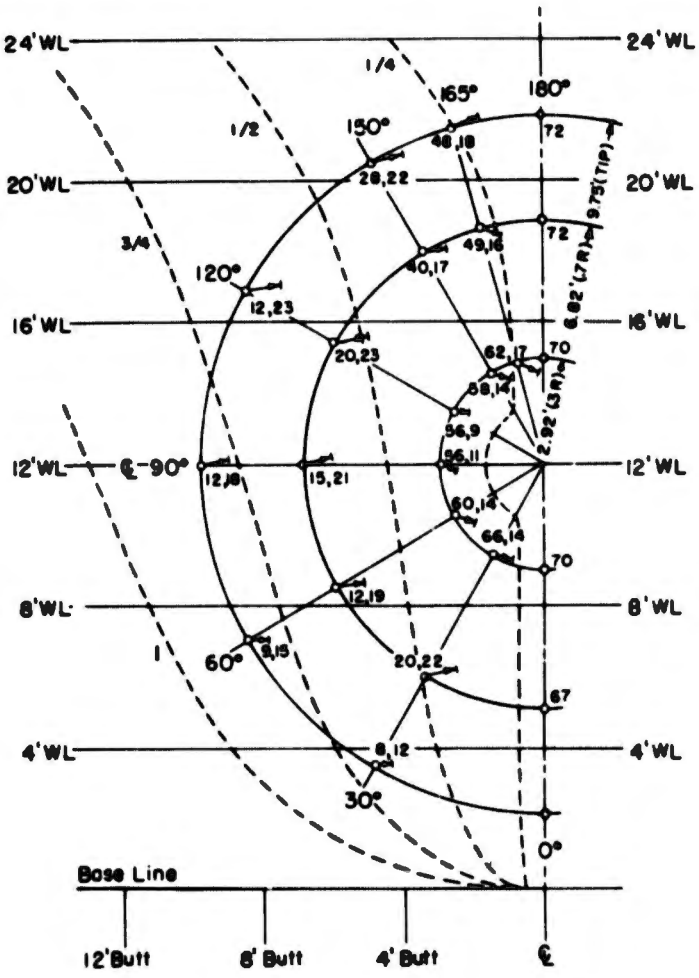


TRANSVERSE SECTION LOOKING FORWARD

Both numerals on the diagram express the magnitude of components of wake velocity as percentages of ship's speed. The first numeral represents the longitudinal component of the wake velocity (longitudinal wake fraction).

The second numeral represents the transverse component of the wake velocity (transverse wake fraction).

The arrow indicates the direction of the transverse wake component.

| | |
|---|---|
| WATERLINE LENGTH = | 513 FT. |
| DISPLACEMENT = | 20,300 TONS |
| DRAFT = | 28 FT 3 IN. |
| TRIM = | 6 IN. BY STERN |
| SPEED = | 15.7 KNOTS |

Wake survey was made along the propeller rake line on three transverse planes:

| | |
|---|---|
| at 0.3R | 6.400 ft forward of AP |
| 0.7R | 5.833 ft forward of AP |
| Tip | 5.416 ft forward of AP |

Appendages:

Bilge keels
Dummy hub
Fairwater

Figure 24a

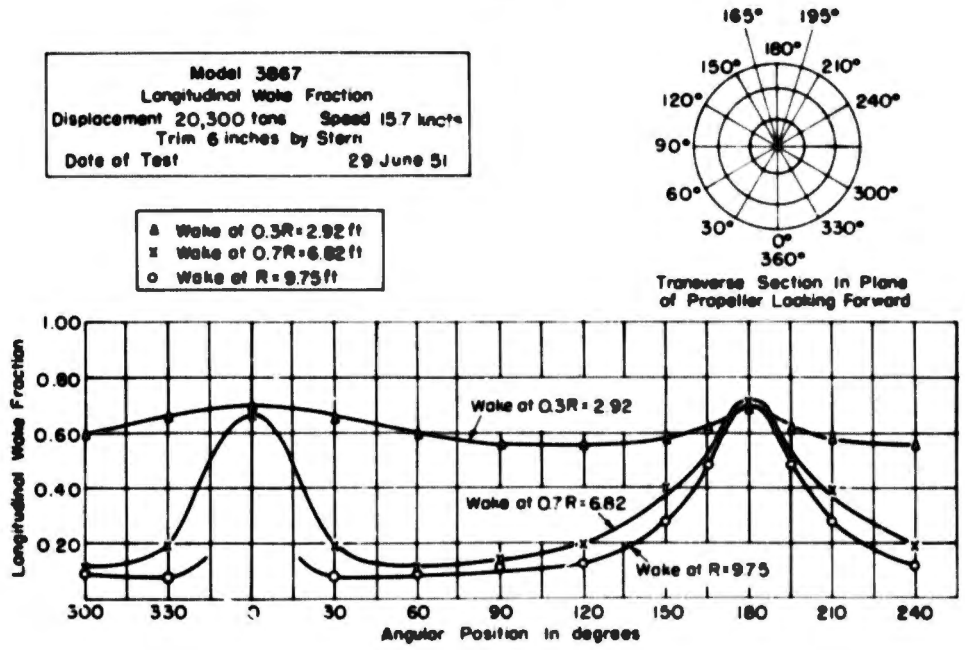


Figure 24b

Figure 24 - Wake Diagrams for T-2 Tanker Model

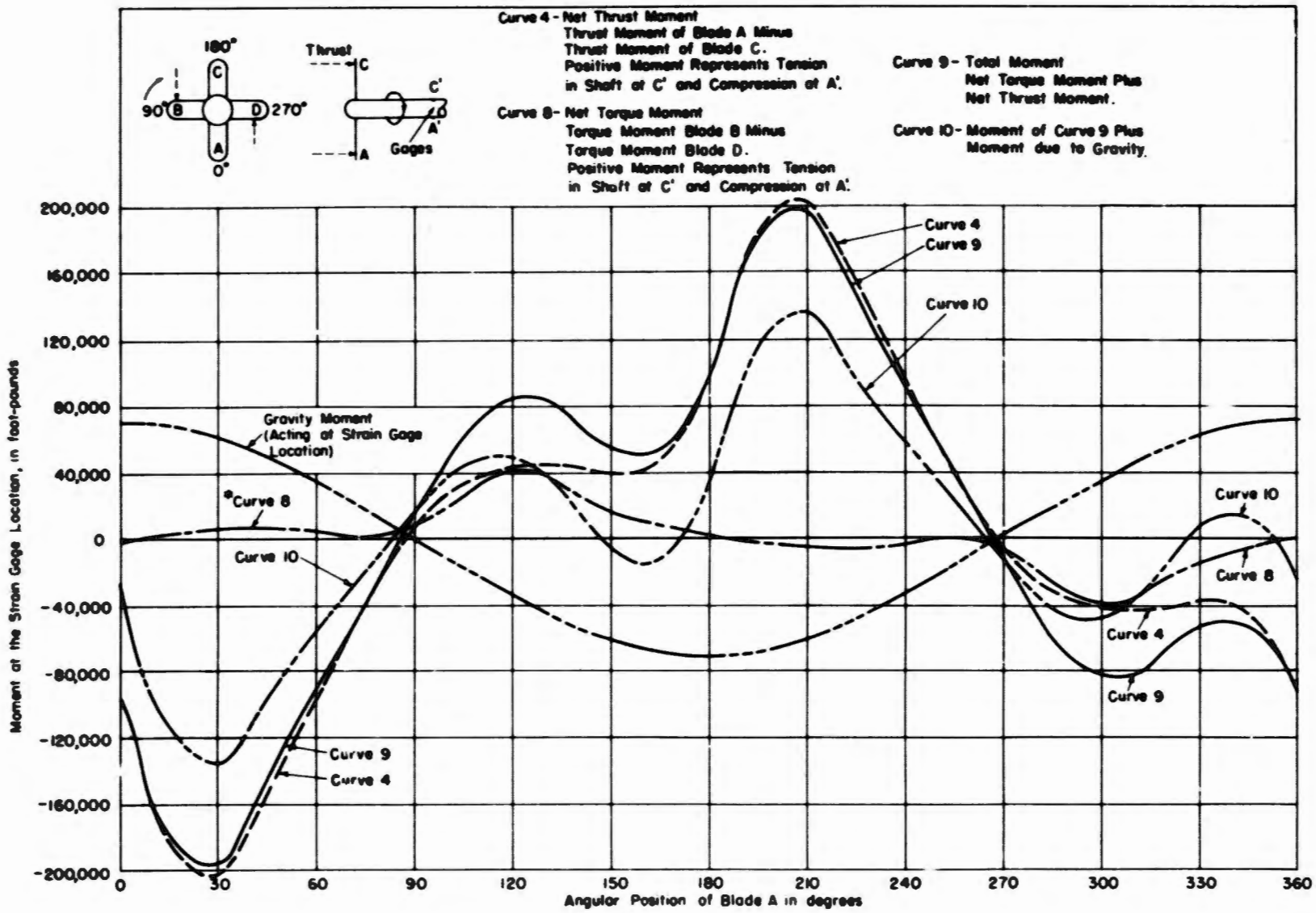


Figure 25a

*Curve 8 - Bending moment at gage locations due to inequality of the forces in the plane of the propeller.

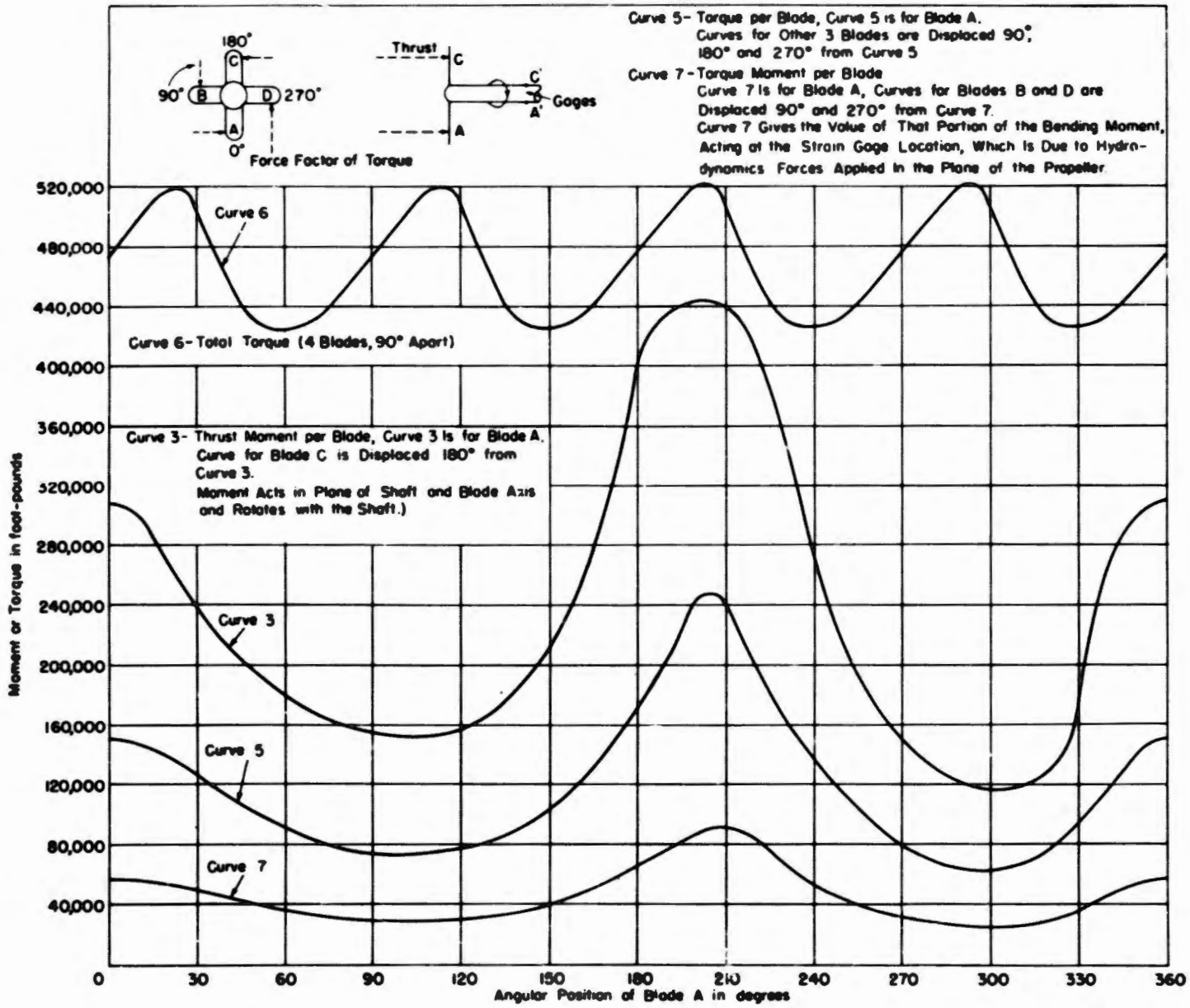
180°
C
90° B D 270°
A
0°
Force Factor of Torque
Thrust
C
C'
D
A'
Gages
A
Curve 5- Torque per Blade, Curve 5 is for Blade A.
Curves for Other 3 Blades are Displaced 90°,
180° and 270° from Curve 5
Curve 7- Torque Moment per Blade
Curve 7 is for Blade A, Curves for Blades B and D are
Displaced 90° and 270° from Curve 7.
Curve 7 Gives the Value of That Portion of the Bending Moment,
Acting at the Strain Gage Location, Which is Due to Hydro-
dynamics Forces Applied in the Plane of the Propeller
Curve 6
Curve 6- Total Torque (4 Blades, 90° Apart)
Curve 3- Thrust Moment per Blade, Curve 3 is for Blade A.
Curve for Blade C is Displaced 180° from
Curve 3.
Moment Acts in Plane of Shaft and Blade Axis
and Rotates with the Shaft.)
Curve 3
Curve 5
Curve 7
Moment or Torque in foot-pounds
520,000
480,000
440,000
400,000
360,000
320,000
280,000
240,000
200,000
160,000
120,000
80,000
40,000
0
30
60
90
120
150
180
210
240
270
300
330
360
Angular Position of Blade A in degrees

Figure 25b

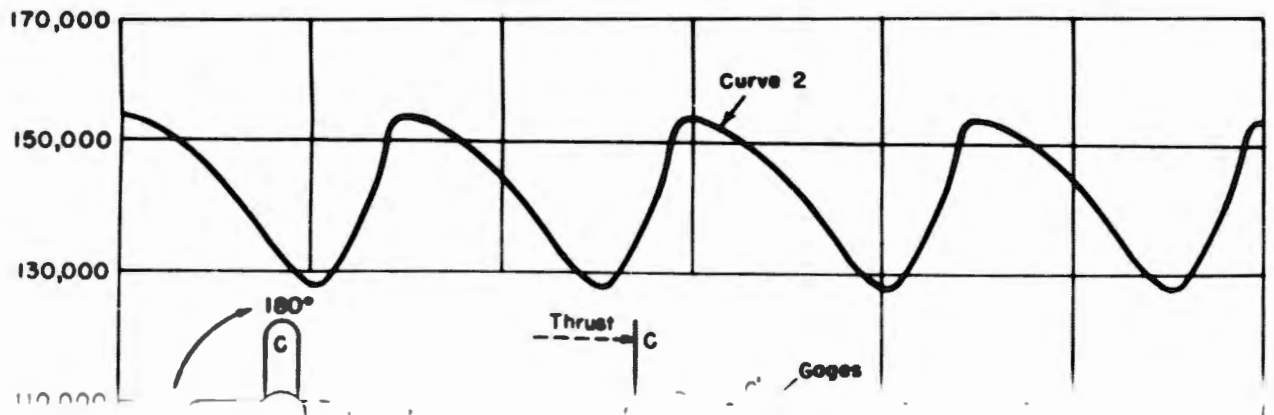
170,000
150,000
130,000
Curve 2
180°
C
Thrust
C
Gages

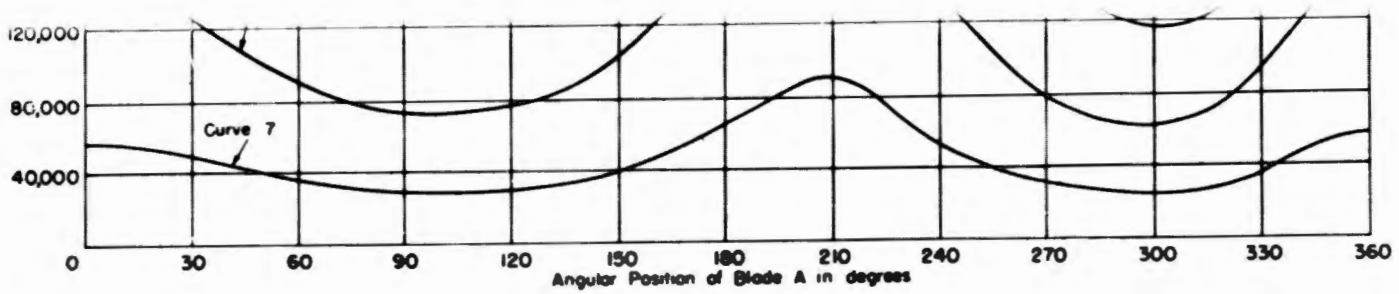


Figure 25b

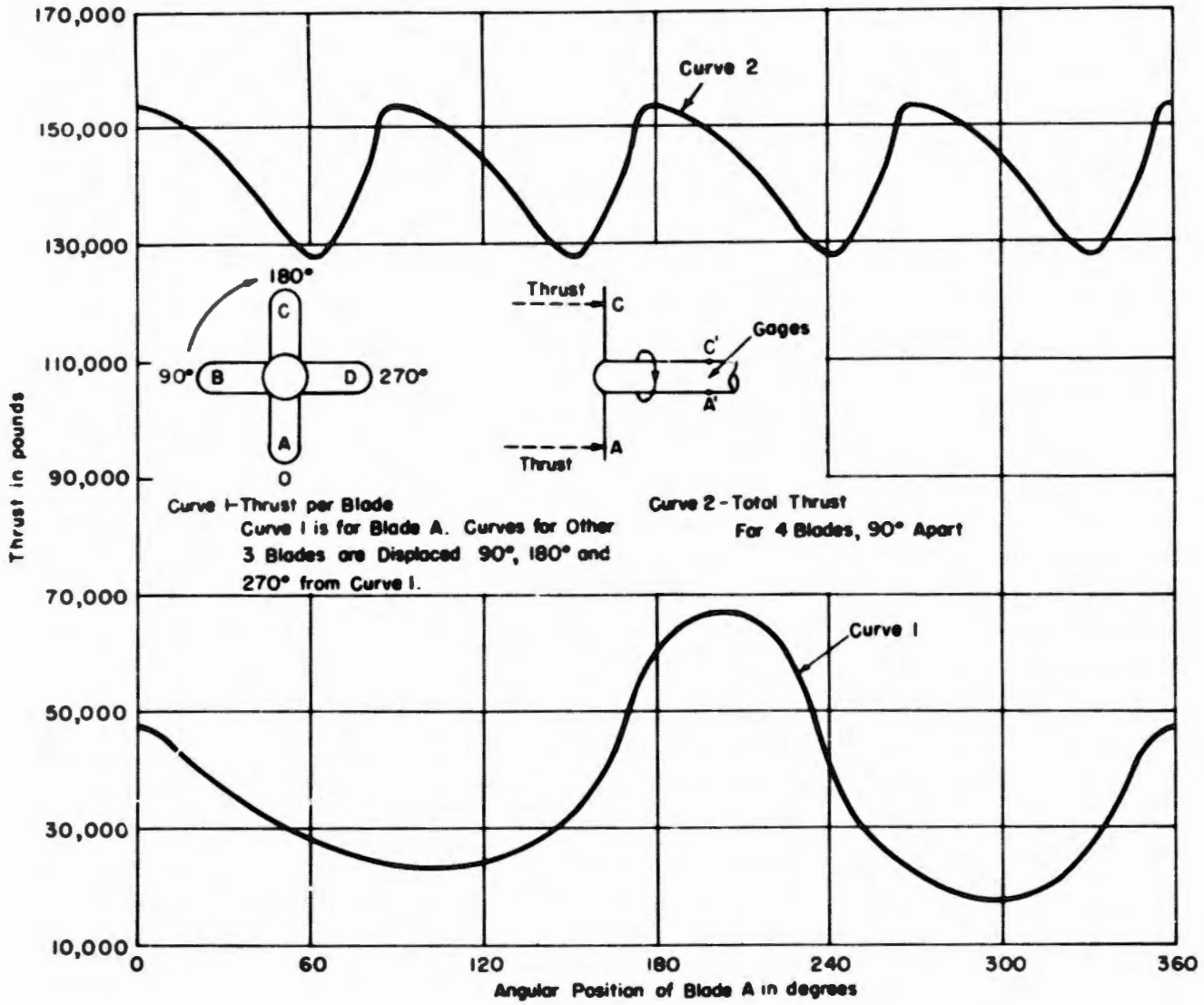


Figure 25c

Figure 25 - Forces and Moments Applied to the Propeller as Computed from Model Wake Tests (95 Shaft rpm)

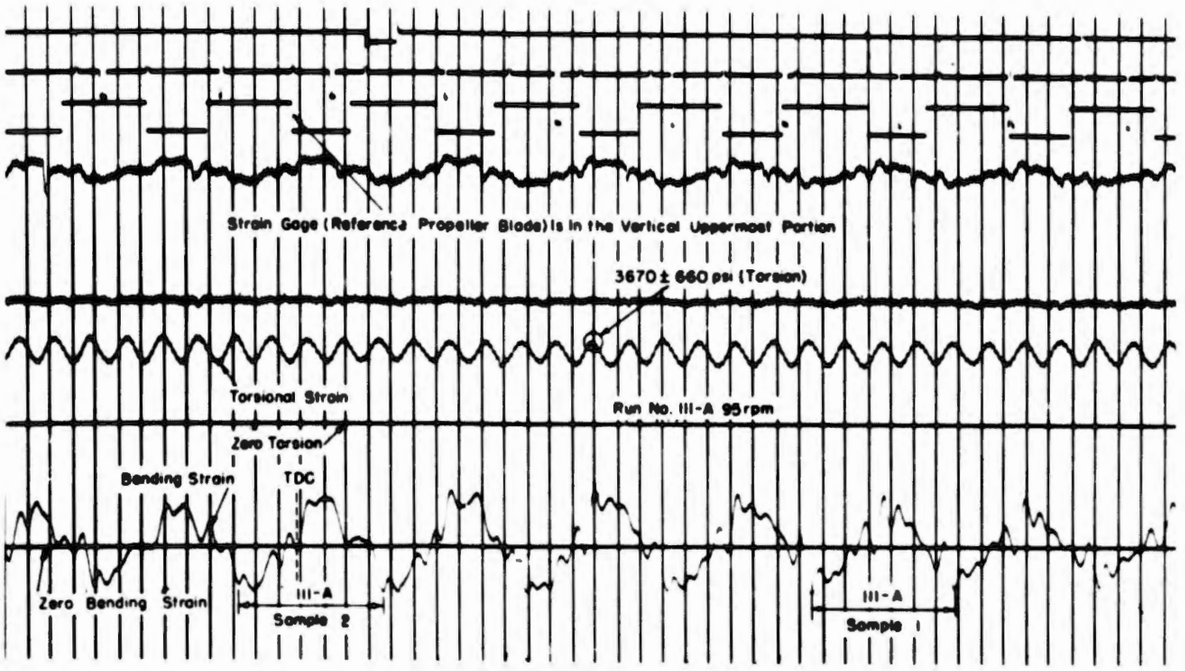


Figure 26 - Strain Oscillogram Taken at 95 Shaft rpm on the T-2 Tanker (Load Condition)

A harmonic analysis of the measured and computed strain variations, shown in Figures 26 and 25, respectively, was made and gave the results shown in Table 8.

The best agreement would be expected in the first-order term with progressively poorer agreement in the higher-order terms. Table 8 does show a reasonable correspondence of the first-order stresses, and, although there is an appreciable variation in the computed and measured third-order terms, their order of magnitude is the same. It may be concluded that, although it

TABLE 8

Comparison of Stresses Computed from Model and Full-Scale Tests

| Quantity | Measured Value T-2 Tanker | | Computed Value from Wake Tests |
|---|---|---|---|
| | Sample 1 Figure 26 | Sample 2 Figure 26 | Curve 10, Figure 25 |
| Maximum Stress | ±1910 psi | ±1850 psi | ±1860 psi |
| 1st-Order Stress Variation | ±1250 psi | ±1530 psi | ±1000 psi |
| 3rd-Order Stress Variation | ±160 psi | ±420 psi | ±840 psi |
| 5th-Order Stress Variation | ±240 psi | ±150 psi | ±300 psi |

does not appear possible to predict with accuracy the bending moment which will act on the shaft, it will be practicable to estimate the service stresses with an accuracy of about 50 percent, excluding resonance effects. The computations necessary for plotting the curves of Figure 25 require approximately one additional day of computer's time, if they are made in conjunction with propeller design computations.

Curve 6 of Figure 25 shows that the model wake tests give a calculated torsional stress of $3730 \pm 730$ psi as against a measured torsional stress of $3670 \pm 660$ psi. Although this seems like excellent agreement, it should be remembered that the measured stresses include the resonance effects. The shaft-propeller system does have a torsional resonance near 90 rpm as discussed previously.

It is suggested that, in the future, curves such as shown in Figure 25 be computed along with the propeller design for cases where the wake diagram does indicate fairly severe wake variations. The data thus obtained should be of value to the shaft designer.

## 6.6. SUMMATION

The tests have shown that the alternating bending and torsion stresses in the shaft were about twice as high during the light displacement condition, in which only about half the propeller disk was immersed, as they were during the load condition. Even for the relatively more severe, light-displacement, steady-speed operation, the normal alternating stresses were only about $\pm 4000$ psi in bending and $\pm 1700$ psi in torsion near 90 shaft rpm. It is, however, a fact that failure does occur with these stresses. Consideration of ordinary stress concentration factors due to geometric discontinuities such as a keyway does not appear sufficient to account for the fatigue failures encountered. The fracture phenomenon, which occurs in these shafts, has its origin in extremely localized sections of the structure and hence is related not only to the average stress, such as is measured by the strain gages, but also to the microscopic aspects of the stress.

The shaft failures are due to a lack of endurance strength of the shaft, and the indications are that the excessive reduction of endurance strength may be primarily due to a fretting action,[16,17,18] which is primarily mechanical in nature, to salt water corrosion, or to a combination of both. The effect of the latter processes is to cause a surface deterioration resulting in high local stresses and progressive fracture. There is no known

conclusive evidence to show that either of these factors is or is not contributing significantly to the shaft failures. It should not be difficult to determine the absence or presence of these effects by examination of propeller shafts that have been in service. G.A. Tomlinson[19] indicates that fretting corrosion depends on the degree of sliding that occurs between two surfaces and that, once a critical value of sliding motion has been exceeded, fretting will take place. If the alternating stresses in the shaft could be reduced, then it is possible that the effects of fretting and salt-water corrosion would also be reduced, although not necessarily in proportion to the stress reduction.

T.L. Oberle[17] discusses the wear of metals and indicates that the wearing ability and the resistance to fretting is a function of the Modell number (Modell No. = Brinell hardness x $10^6$/modulus of elasticity) and is greater the higher the Modell number. It is thus possible, according to this theory, if the end of the shaft sleeve or of the propeller does move relative to the steel shaft, under vibratory stress, that the lower modulus composition will wear the shaft (fretting) providing that its Modell number is higher than that of the shaft.

Another factor which may have bearing on the reduction in endurance limit is the effect of temperature on the endurance strength. It has been shown that the notch sensitivity of steels, under static load application, is greatly increased as the temperature is lowered. It is not unreasonable to assume that a similar effect may be present under vibratory load conditions. It is, of course, possible that the tailshafts may be subjected to fairly low temperatures depending on the routes traveled.

The measured bending strain variations do show the presence of higher-order whirling motions; actually eighth-order whirling resonances are indicated near 90 and 105 shaft rpm (Figure 21b), and since the measured resonance frequency of the counterwhirl is lower than that of the forward whirl it is concluded that these whirling motions are significantly affected by the gyroscopic effect of the propeller, in accordance with the theory of Section 6.1 and Reference 11.

The third-order bending strain variations (fourth-order forward whirl), although the largest magnitude higher-order strain variation present, did not pass through a resonance throughout the speed range, i.e., up to 110 shaft rpm, contrary to the theory proposed by Mr. Panagopulos.[5] It can be stated, therefore, that a fourth-order resonant whirl does not occur on this ship. The model wake study also indicates the presence of a strong third-order moment variation, referred to a point fixed in the shaft; consequently, a strong third-order bending strain is to be expected. The predominant bending

strain variation, in both the light and heavy displacement conditions, was of shaft rpm frequency and would be present to some degree due to the effect of gravity, regardless of any other excitations.

A torsional resonance of the shaft occurred within the operating speed range of the vessel (90 rpm). This torsional vibration is excited by the fourth-order torque component due to the wake variation. Operation of the vessel which permits the propeller blades to emerge from the water greatly increases the magnitude of the alternating stresses.

The tanker tests have shown that a trim of the ship which will allow only partial immersion of the propeller should be avoided since such a condition will result in a considerable increase in all vibratory stresses in the shaft.

The solution to the shaft failure problem of these ships is to be sought in increasing the endurance strength of the shaft primarily by attention to those factors which cause a surface deterioration of the shaft such as fretting and salt-water corrosion (galvanic action). It should be emphasized that, in the presence of vibratory stresses, both fretting and salt-water corrosion can give rise to large, highly localized stresses incident to the surface deterioration which accompanies these processes, even though macroscopic strains, as measured with strain gages, are quite small.

In future hull designs it would be advisable to study the wake variation over the propeller disk and to make a strong effort towards a reduction of the moment variations which act on the propeller disk.

## 7. CONCLUSIONS

1. The failure of tailshafts cannot be ascribed to a single factor. The study of the problem requires a rather complex analysis.

2. The propeller-shaft system does not have a fourth-order whirling resonance within the speed range of the ship. There is experimental evidence of an eighth-order forward whirling resonance at 840 cpm and an eighth-order counterwhirl resonance at 720 cpm, excited at 105 and 90 rpm, respectively. These modes are believed to be the fundamental modes of whirling vibration in view of the fact that the frequencies are of the order of magnitude of the natural frequencies of flexural vibration of the nonrotating shaft, immersed in water, as experimentally determined by means of vibration-generator tests.

3. The bending stress variations in the tailshaft are due primarily to external bending moments applied to the propeller as well as to the gravity effect of the overhanging weight of the propeller. A smaller but significant

contribution to the bending stresses is caused by the resonant eighth-order whirling motion of the shaft.

4. The torsional shaft vibration does have a fourth-order resonance of about 360 cpm, which occurs at 90 shaft rpm. The torsional stresses are increased considerably owing to the effect of resonance.

5. The magnitude of both bending and torsional vibratory stresses is increased appreciably when the vessel is trimmed so as to permit the propeller blades to emerge from the water (ballast condition). For the test conditions existing on the MISSION SAN LUIS OBISPO the vibratory stresses were approximately doubled when the ship's propeller was only partially immersed. In the latter case the bending moment due to the propeller overhang and that due to eccentric thrust application are additive whereas they tend to cancel one another when the entire propeller is immersed.

6. The alternating component of the stresses measured during the light displacement condition were about $\pm 4000$ psi in bending and $\pm 1700$ psi in torsion at 90 rpm (see Tables 4 and 5 for a compilation of these stresses).

7. A rough prediction (within about 50 percent accuracy) of the forces and moments applied to the propeller and the consequent stresses in the propeller shaft can be made on the basis of an analysis of a model wake test, provided no significant resonance effects will occur.

8. The shaft failures are due to a lack of endurance strength of the shaft assembly.

9. The indications are that the excessive reduction of endurance strength of these shafts may be due primarily to a fretting action, to salt-water corrosion (galvanic action), or to a combination of both. It is not unlikely, furthermore, that the endurance strength of steel may be adversely affected at low temperatures. In order for failure to result from these actions they must be accompanied by vibratory strains.

10. The formulas given by the Bureau of Ships Design Data Sheets[15] for the strength design of shafts are not safe for general use. They should be modified, possibly along the lines suggested in Section 6.4, or else the shaft design should be changed to eliminate indeterminate effects such as fretting corrosion.

11. The gyroscopic effect of the propeller disk does play an important role in determining the natural frequencies of flexural vibration (whirling motion) of propeller-shaft systems at the low shaft revolutions encountered in ships as well as for high-speed rotors.

12. The flexibility of the bearing supports of the tailshaft-propeller system may vary appreciably along different radial directions as indicated by vibration-generator tests of these systems. For the T-2 tanker tested, the over-all stiffness of the system in the vertical plane is about 1.5 times that in the horizontal plane. Similar tests on a Liberty ship indicate that, in this case, the corresponding stiffness ratio is about 2.5.

13. The computation of the flexural resonance frequencies of a rotating propeller shaft must take the flexibility of the bearing supports into consideration. A relatively simple method for making such computations is indicated in Section 6.1. To obtain reasonably accurate values for these frequencies it is necessary to determine the type and the stiffness of the bearing supports.

14. Very little is known as to the endurance strength under combined stresses such as occur in the tailshaft.

15. The general pattern of bending strain variations and flexural vibrations encountered on the T-2 tanker will probably be applicable to the Liberty ships.

## 8. RECOMMENDATIONS

1. The endurance strength of the tailshafts should be increased. This may be accomplished, in part, as follows:

a. Reduce obvious stress concentration factors by rounding off sharp corners in the keyway, etc.

b. Determine whether a fretting action exists between the edge of the shaft sleeve or propeller hub and the shaft by making a metallurgical examination of condemned shafts or of shafts that have had considerable service. This should be relatively easy to accomplish. If a fretting action is present, its effects may be alleviated by adjusting the Modell numbers (Reference 16) of the mating surfaces to decrease the surface deterioration of the steel, by preventing the relative motion between the mating surfaces or by elimination of the composition sleeve. Reference 17 contains a discussion of remedial actions. The possibility of cladding ordinary steel shafts with a fretting and corrosion-resisting material might be considered. The possibility of utilizing a rubber-covered steel shaft should be studied. Cold rolling or nitriding of shaft in way of press fits has been suggested for reducing effects of fretting.

c. Determine whether salt-water corrosion (galvanic action) of the shaft does occur. This may be ascertained from a metallurgical inspection of condemned shafts. If salt-water corrosion does occur, it must be eliminated or else a minimum useful shaft life must be accepted. Exclusion of salt water from the steel shaft would necessitate development of better sealing methods and more rigid control over shaft-installation procedures. A more direct solution would be replacement of the steel shaft by a stainless steel shaft or by a steel shaft with a cladding of a corrosion-resisting material.

2. It is recommended that a study be made of the effects of low temperatures on the endurance strength of steel in the presence of representative types of surface discontinuities. Such a study may bear results similar to those obtained from the study of the variation of notch sensitivity with temperature under gradually applied loads.

Some effort should be expended to learn more about the endurance strength of steel under combined stresses such as do occur in the tailshaft.

3. The shaft design procedures of Reference 15 should be modified as follows:

a. In addition to a computation of the bending moment resulting from the overhanging propeller, the bending moments due to the condition of most severe wake variation to be expected in service, should be considered. The latter values may be obtained from an analysis of model wake tests, such as is presented in Figure 26. Alternatively, an approximation may be made by representing the effect of the wake variation by a series of eccentric applications of different orders of thrust variations. For the sake of convenience, representative data for various classes of ships could be tabulated to give an equivalent eccentricity for each significant order of moment variation which, if multiplied by the mean propeller thrust, would give the magnitude of the desired order of moment variation. This equivalent eccentricity should probably be given as a fraction of the propeller diameter.

b. The calculation of the natural frequency of flexural whirling vibration of the propeller-shaft system should consider the flexibility of bearing supports as well as rotary inertia and gyroscopic effects of the propeller. A method which does this and yet is not too complex for practical application by engineers is outlined in Reference 11. Information as to the type and stiffness of

the shaft supports is rare, but essential for frequency calculations. Such data should be collected by means of full-scale tests.

c. The lowest nth order whirling resonance of the propeller shaft (where n is the number of propeller blades) should lie outside the operating speed of the shaft.

d. The calculation of the endurance strength of the tailshaft should be modified as indicated in Section 6.4, Equations [3] and [4].

5. Systematic tests should be made on typical ship installations in order to determine the type and stiffness of the tailshaft supports. Comparison of computed and measured natural whirling frequencies should be made whenever the opportunity presents itself.

6. Ships should be operated at a condition of trim which will insure immersion of the propeller. If it is known in the design stage that loading requirements do not permit such operation, then the shaft design should be checked as indicated in Recommendation 4a.

7. Stress raisers associated with the presence of a keyway and a forced fit between shaft and propeller hub may be eliminated by utilizing a bolted connection between shaft and propeller. The advantages and disadvantages of such an arrangement should be evaluated.

8. Every effort should be made to keep the vibratory stresses in all parts of the shaft system to a minimum and to prevent vibratory relative motions between mating surfaces because the deleterious effects incident to such stresses and motions are rather unpredictable and may be out of proportion to the severity of the vibratory strains relative to the static strains. Vibration appears to be an essential factor in the process of fretting corrosion.

## ACKNOWLEDGMENT

The study presented in this report is the result of the efforts of many people. Mr. E. Panagopulos was responsible for stimulating the initiation of this project.

The Bureau of Ships, with the cooperation of a panel set up by the Society of Naval Architects and Marine Engineers to investigate the shaft failures, formulated a general program of which the present study, made by the Taylor Model Basin, is an important part. The efforts of the panel members,

especially of CDR Rupp, Mr. McGoldrick, Mr. Panagopulos and Dr. Baker, in behalf of this project are hereby acknowledged. Mr. E. Noonan of the Bureau of Ships was instrumental in setting up the projects at the Taylor Model Basin under which the full-scale investigations, here discussed, as well as laboratory and theoretical studies on the flexural vibrations of shafts are being carried out.

The instrumentation of the shaft was accomplished by members of the Electronics Engineering Division at the Taylor Model Basin. Mr. Wilner, of the Model Basin staff, advised the author on the metallurgical aspects of the problem. The following members of the Vibrations Division assisted in obtaining and analyzing the test data, Messrs. J.T. Birmingham, H.D. Messer, Q.R. Robinson and Mrs. A.W. Mathewson. The model wake test, as well as the computation of the applied moments due to the wake, were made by the Propellers Section of the Taylor Model Basin. Dr. E.H. Kennard, Chief Scientist of the Structural Mechanics Laboratory, and Mr. McGoldrick of the Vibration Division made valuable suggestions in connection with the study of the whirling motions of shafts. The vibration measurements reported in the Appendix were made by representatives of the General Electric Company. The study presented in this report was made by the author.

# APPENDIX

## VIBRATION MEASUREMENTS MADE BY THE GENERAL ELECTRIC COMPANY

The General Electric Company installed displacement gages at the after end of the after stern tube bearing and at the after end of the first inboard line bearing for the purpose of measuring the vertical and horizontal motion of the shaft relative to the ship. In addition, a portable vibration pickup was used to measure the vertical and horizontal vibratory motion of the shaft midway between the first inboard line bearing and the stuffing tube (see also Figures 6 and 8).

Sample oscillograms of these motions are shown in Figure 27, and a rough analysis of the oscillograms is given by the graphs of Figure 28.

Only limited information can be gathered from these data due to a combination of circumstances, for example:

A. Two of the pickups (Traces E and F of Figure 27) were located next to the first inboard line bearing, and since a bearing does, of course, restrict the motion of the shaft, the measured whirling motion at such locations is relatively small. Any out-of-roundness or runout of the shaft will be measured by the pickup, see for example, the first-order motion of Traces E and F of Figure 27.

B. Two pickups (Traces C and D) were located just aft of the after stern tube bearing; the comments under A preceding apply to some extent to this location. Furthermore, much greater amplitudes of motion than actually measured had been expected, and consequently the actual signal strength during the tests was quite low, resulting in very small deflections of the oscillograph trace, which made accurate analysis impractical.

C. All the motion measurements may include, to some extent, the effects of out-of-roundness of the shaft and of hull vibrations.

The motion measurements do not indicate definite resonances; however, they do confirm the presence of strong fourth- and eighth-order whirling motions. The pickups located at the inboard line bearing evidenced strong eighth- and fourth-order motions during the light load condition only, with only partial immersion of the propeller; during the load condition first-order vibrations predominated at this location. The actual hull vibrations near the fantail were of the order of 1 mil single amplitude; therefore, it is not likely that the data plotted in Figure 28 are appreciably affected by the hull vibration.

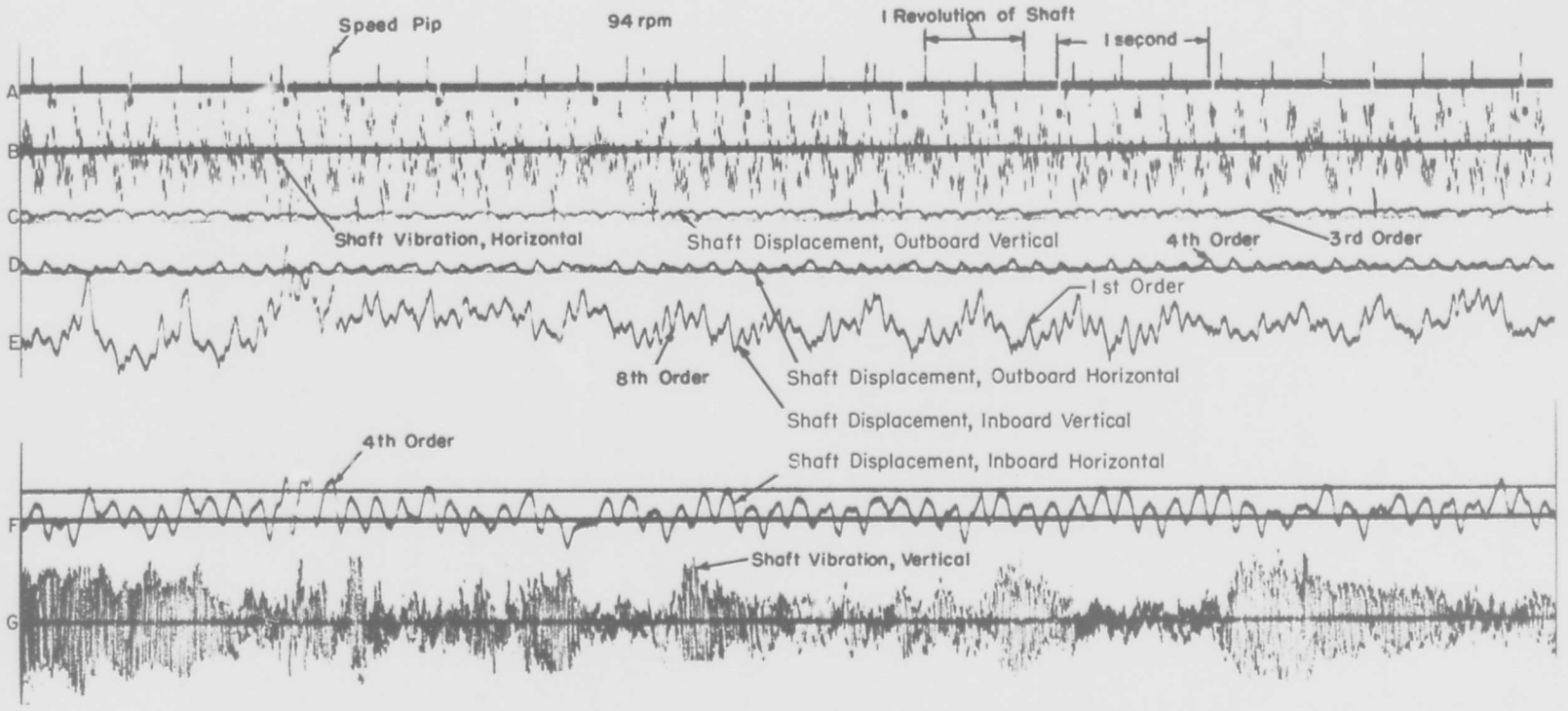


Figure 27 - Sample Records of Vibration Measurements Made by the General Electric Company on the MISSION SAN LUIS OBISPO

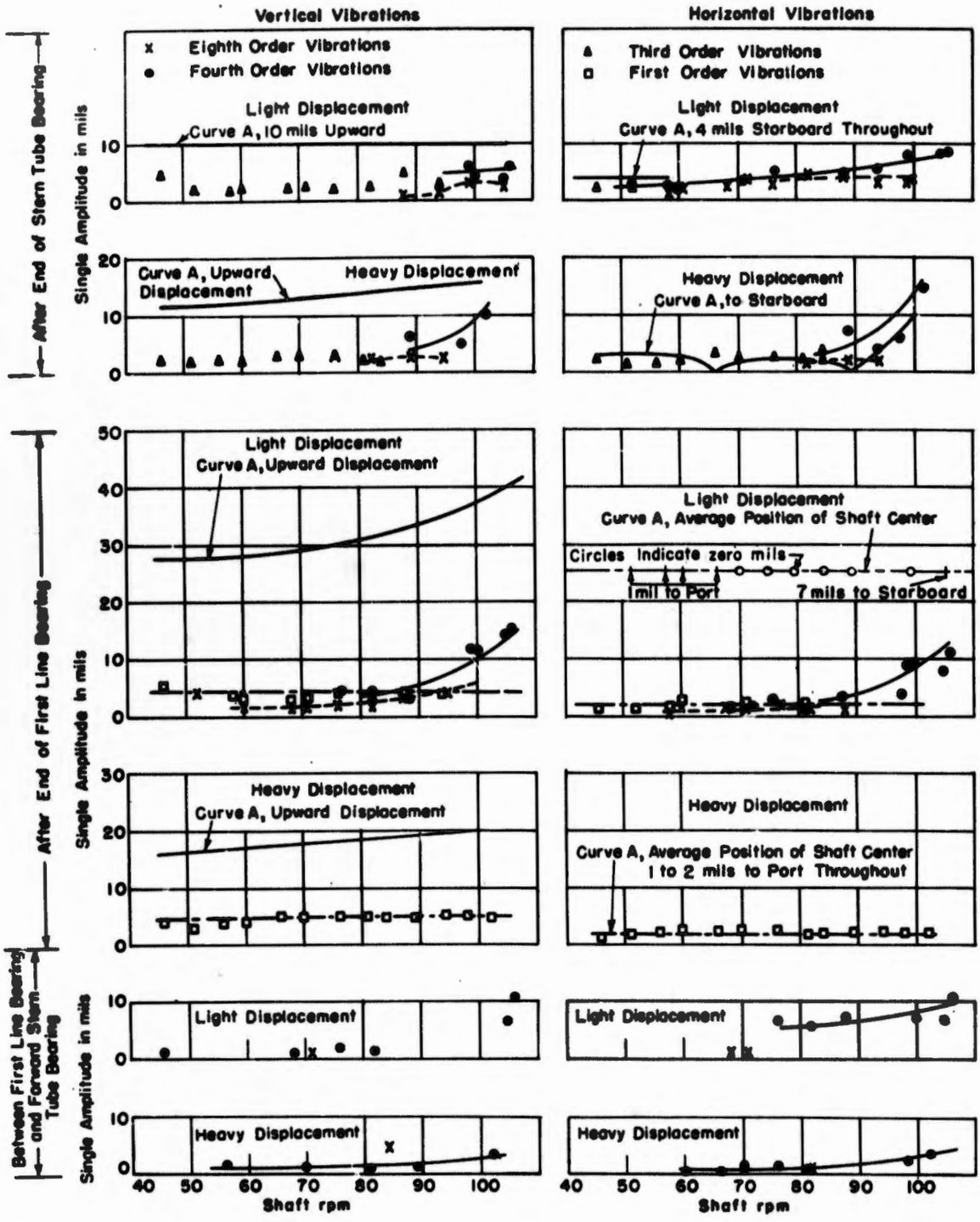


Figure 28 - Shaft Motion Data Obtained from Measurements Made by the General Electric Company on the MISSION SAN LUIS OBISPO

Curve A gives the average position of the shaft center.

The one disconcerting item in these vibration data is the rather definite third-order vibration occasionally measured at the outboard bearing. Theoretically, there should be no third-order whirl. However, a possible explanation is as follows: A first-order forward whirl is caused by the presence of mass unbalance in the shaft and in the propeller; a fourth-order counterwhirl is generated by the hydrodynamic forces as discussed in the body of the report. If the two whirls have the same amplitude, their sum would be equivalent to a third-order whirl. The third-order vibration was not steady in character, and, if the records were such as to permit making a harmonic analysis, both first- and fourth-order components would probably be obtained.

In general, the effect of these displacement measurements is to confirm the analysis made on the basis of the strain measurements, although the motion data in itself would not have provided a clear picture of either the motions of or the stresses in the shaft.

## REFERENCES

1. BuShips ltr S43-1(371) Serial 371-57 of 27 June 1950 to TMB.

2. BuShips ltr S43/1(371) over Serial 371-141 of 21 March 1951 to TMB.

3. Archer, S., "Screwshaft Casualties - The Influence of Torsional Vibration and Propeller Immersion," Transactions INA, 1949.

4. Gatewood, A.R., "Some Notes on Propeller Shaft Failures," paper presented before the New York Metropolitan Section of the SNAME, April 27, 1950.

5. Panagopulos, E., "Design Stage Calculations of Marine Shafting," Trans. SNAME 1950, Vol. 58.

6. Jasper, N.H., "Structural Vibration Problems of Ships - A Study of the DD692 Class of Destroyers," TMB Report C-36, February 1950.

7. Sawyer, W.T. and Dunford, J.M., "Investigation of Factors Affecting the Flexural Critical Speed of Propeller Shafting," A thesis submitted for the degree of Master of Science from MIT, October 1944.

8. Jasper, N.H., Discussion of "Design Stage Calculation of Marine Shafting," pp. 370-373, Trans. SNAME, 1950.

9. Stodola, A., "Steam and Gas Turbines," Vol. II, pp. 1110-1112, translation by Dr. L. Loewenstein, published by Peter Smith, New York, 1945.

10. Timoshenko, S., "Vibration Problems in Engineering," Second Edition, D. Van Nostrand Company, July 1937.

11. Jasper, N.H., "Critical Whirling Speeds of Shaft Disk Systems (Propeller Shaft System)"TMB Report 827 in preparation.

12. New York Naval Shipyard ltr 941:WHK:tw over S43/1/L5, Lab Project 5078-1, of 8 June 1951 to TMB.

13. "The Lazan Oscillator Model LA-1, Instructions for Installation, Operation and Maintenance," The Baldwin Locomotive Works, Phila. 42, Pa.

14. Soderberg, C.R., "Working Stresses," Trans. ASME, Vol 55, 1933, APM-55-16.

15. BuShips Design Data Sheet DDS 43-1, Part 1, 1 December 1944.

16. Godfrey, Douglas, "Investigation of Fretting by Microscopic Observation," NACA Report 1009, 1951.

17. Oberle, T.L., "Wear of Metals," Journal of Metals, June 1951, pp. 438-439.

18. Albert, E.V., "Do You Know About Fretting Corrosion?" Diesel Power and Diesel Transportation, March 1949.

19. Tomlinson, G.A., Thorpe, P.L. and Gough, H.J., "An Investigation of Fretting Corrosion of Closely Fitting Surfaces," Institute of Mechanical Engineers Proceedings, 141: pp. 223-237, 1939.

NAVY-DPPO PRNC WASH D.C